UNIVERSITY OF
BIRMINGHAM

On-Line Monitoring of Rheology using Passive Acoustic Emission with Machine Learning

BY

Temilade Ayinde-Tukur

Thesis submitted to the
University of Birmingham
for the degree of
MASTER OF RESEARCH

School of Chemical Engineering
College of Engineering and Physical Sciences
University of Birmingham
March 2022

Acknowledgements

The effort and grace to undertake and complete this research work stems from the Almighty God who "works in [us] to will and to do for His good pleasure" (Philippians 2:13).

"Think what God has determined to do to all those who submit themselves to His righteousness and are willing to receive His gift." – James C. Maxwell; June 23, 1864.

Immense gratitude goes to my primary supervisor, Dr Federico Alberini, for his dedication and support throughout the lifecycle of this project, my secondary supervisor, Dr Richard Greenwood, for providing valuable support towards putting the entire research project report together and Cyrus Espinoza who helped me get up to speed with the technology and was always willing and available to support when needed.

Special acknowledgement to my son, Joshua, who struggled medically throughout the duration of this project but still put up a cheerful and courageous face through it all and to my pillars of support, Daniel and Adetoro, without whom this might not have been possible. Final acknowledgements to my family for their continuous support.

ABSTRACT

Global technological advancements in manufacturing through automated and intelligent systems provide opportunities for leaner, more efficient and higher quality production processes. In the manufacture of liquid products that rely heavily on rheological parameters to provide insight into the quality of such products, being able to implement an automated and intelligent cyber physical system can prove very valuable in industry. In the continuous race to optimise techniques and tools used in monitoring and measuring rheology, the rheometer has evolved from a mechanical viscometer to fully automated rheometer providing real-time process data. However, these automated systems can become quite complex and expensive. This research work investigated the viability of a simpler, non-invasive, cyber physical system comprising of a passive acoustic emission sensor that collects acoustic data in real-time from the fluid in a process, along with a set of mathematical models and machine learning algorithm that converts the data into rheological fingerprints. These rheological fingerprints can then be used to monitor a live manufacturing process or can be further used to develop a stored frequency database for measuring rheological values through the principle of inference.

The use of a non-invasive, relatively simpler technology such as the passive acoustic emission sensor provides flexibility in functionality as the cyber physical system is able to measure and monitor other fluid properties simply by changing the mathematical models used for data processing. This research work makes use of a closed loop flow piping setup to mimic a continuous manufacturing operation process and investigated the monitoring of rheology of Glycerol, Carboxymethyl Cellulose and Carbopol® solutions to represent Newtonian, Power Law and Herschel-Bulkley types of rheology. Reference rheological values for these fluids first obtained on a standard offline rheometer served as output values while the processed acoustic rheology data served as input values to then be used to train a predictive function using Artificial Neural Network (ANN) algorithms. This research work shows that the online rheology monitoring system is able to distinguish between changes in a fluid's rheology by picking up distinct acoustic waves and these distinctions can be visually represented as rheological fingerprints using mathematical models to serve as a visual monitoring tool and even further developed into a predictive model function that can estimate unknown rheological values.

Table of Contents

Table of Figures

Table of Tables

1 INTRODUCTION

1.1 INDUSTRY 4.0 AND ARTIFICIAL INTELLIGENCE IN MANUFACTURING

Industrial and technological evolution in the manufacturing industry can be marked by four key milestones to date. The 18th Century marked the introduction of steam powered engines to usher in the First Industrial Revolution. By the late 19th Century, the manufacturing industry had evolved into mass production and the introduction of electricity powered machines to mark the Second Industrial Revolution. The Third Industrial Revolution saw the introduction of automation to manufacturing and the use of electronics and robotics by the start of the 20th Century. The 21st Century has now seen electronics, robotics and the use of information technology in manufacturing advance to become the Fourth Industrial Revolution where artificial intelligence and smart factories merge both the physical and digital world (Schwab, 2016).

The Fourth Industrial Revolution, also known as Industry 4.0 is built on the back of four major principles, namely

i. Internet of Things (interconnection);
ii. Big Data (information transparency);
iii. Automated Tasks; and
iv. Autonomous systems (decentralised decision making) (Habib & Chimsom, 2019).

Figure 1-1 shows the technologies that make Industry 4.0 possible. Processes and systems are able to transfer information amongst each other through the use of sensors and devices enabled by the Internet of Things. Big Data enables the vast amount of data running through the network to be stored, analysed and easily accessed. Data Science in Big Data serves as a major enabling technology by being able to process, analyse and extract knowledge from data using machine learning algorithms that identify patterns and anomalies in the data set. This knowledge then enables these digital systems to predict outcomes and make decisions.

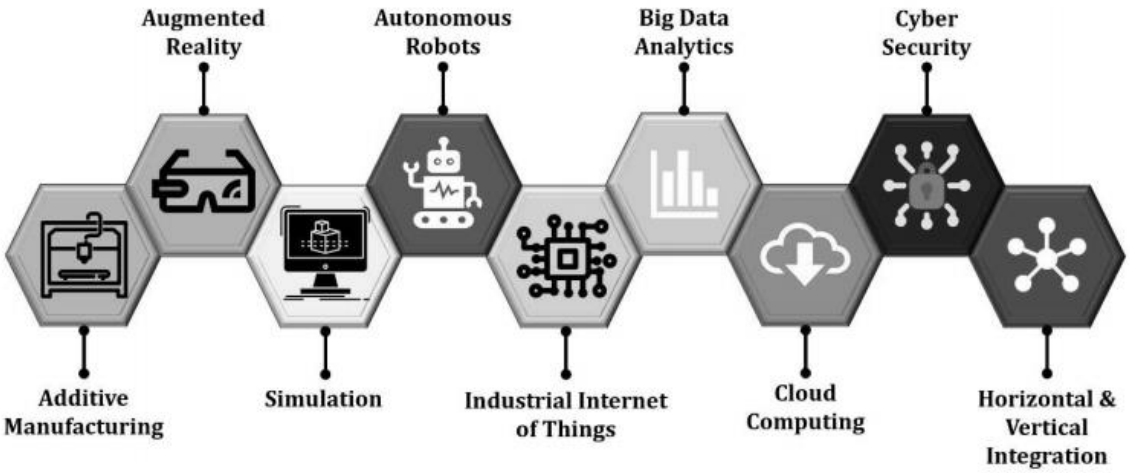

Figure 1-1: Enabling Technologies of Industry 4.0 (Javaid, 2020)

In Manufacturing, Internet of Things (IoT) which enables the transfer of information is also called Industrial Internet of Things (IIoT) and both terms can be used interchangeably. Industrial Internet of Things enables interconnection of the entire supply chain by allowing

visibility end to end from demand forecasting to supply execution and back to demand optimisation. IIoT connected factories make use of cyber physical systems to provide real time data on production line operations, material and inventory levels, quality control and release of products, asset availability and performance, maintenance management, warehouse utilisation and logistics optimisation to bring together both the physical and digital world in a manner that delivers quantifiable value to the manufacturing industry. This, in turn, optimises the entire supply chain to deliver improved productivity levels and increased efficiencies across board, enhance knowledge sharing between core components of the supply chain and enable faster response and better collaborative efforts which deliver greater agility, flexibility and ultimately, higher cost performance and better revenue margins for the company (Javaid, 2020).

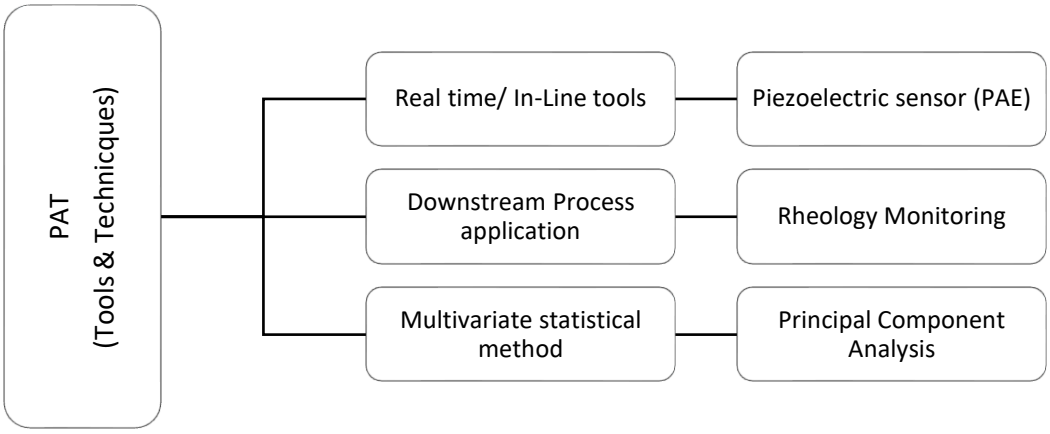

Figure 1-2: Process Analytical Technology schematic for Rheality™ (Misra, Sullivan, & Cullen, 2015)

This research work investigates the use of a smart physical device to develop a system for on-line, real time monitoring of rheology using an acoustic sensor and machine learning tools. The patented Rheality™ technology is a non-invasive monitoring system which uses passive acoustic emission measurements captured by a piezoelectric sensor and processed using machine learning algorithms to generate a sample frequency spectrum that can then be correlated to a database of stored frequency spectra, using artificial intelligence, to provide visual, real time monitoring of product rheology in the manufacturing process. The piezoelectric sensor is placed in-line, which is directly on the external part of the pipe so it does not come in direct contact with the fluid. The raw data is collected in its time domain by the sensor then processed using multivariate data analysis and a schematic of its Process Analytical Technology (PAT) is shown in Figure 1-2 where the tool to be used is identified as the piezoelectric sensor, process application is rheology monitoring and statistical method employed is principal component analysis.

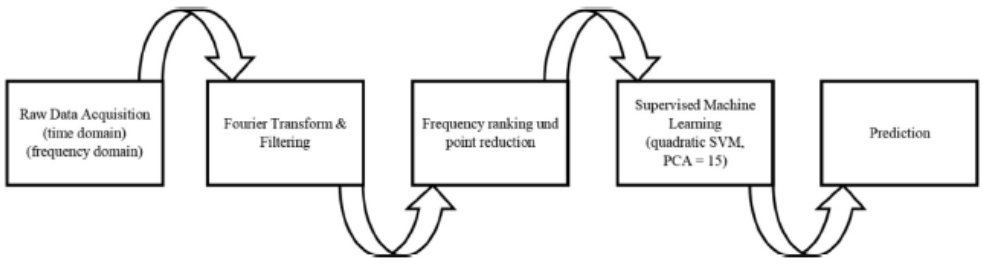

Figure 1-3: Schematic of the AI technology used by Rheality™ (Hefft & Alberini, 2020)

Figure 1-3 shows the schematics of AI technologies that enable the Rheality™ technology. The data is collected in its time domain and converted to its frequency domain using Fast Fourier Transform, then using principal component analysis, the sampled frequency spectrum is apportioned into a plurality of sections with each section being defined by a parameter that can be considered to represent a rheological factor for a particular fluid. These parameters or Rheality™ Rheological Factors (RRF™) are then put in a matrix to predict the rheological values for unknown fluid using supervised machine learning. (Hefft & Alberini, 2020)

Rheology is the study of a materials resistance to flow and understanding deformation of materials (Darby, 2001). For liquids, the measure of frictional force to be overcome in order to move the liquid can be described as the liquid's resistance to flow or viscosity (Malkin & Isayev, 2012). The rheology of raw materials as well as formulation mix of personal care products such as shampoos, soaps, lotions is a key parameter to performance and quality, and traditionally, rheology is measured using offline viscometers or rheometers. The use of rheometers in manufacturing has evolved over time from the mechanical viscometers to electrical rheometers that can measure more rheological properties of fluids besides viscosity (Barnes, 2000). Measuring rheology with traditional rheometers imply that a sample is taken off the processing line for measurement, and in a continuous manufacturing environment, data obtained from offline processes tend to differ from actual because the rheology of the material is highly likely to have changed from the time of sampling so being able to measure and monitor rheology in real time is of essential value. These electrical rheometers which are normally standalone devices have also been developed to in-line and online rheometers to bring rheology measurements real-time in manufacturing. The ability to monitor and possibly measure the rheology of liquid products with complex formulation present an opportunity for a quicker response to formulation changes, defect detection and quicker release times by providing a lot of insight into the extent of mixing, dosage levels and stability of the product.

This project makes use of an experimental rig setup as a simple continuous flow loop with a pump and vessel to mimic a continuous manufacturing process. The acoustic signal data of sample fluid pumped through this closed loop system will be captured using a non-invasive, passive acoustic sensor and the data collected will be processed with a data analytical software to generate a frequency fingerprint for the fluid which is a marker of the rheological characteristics of the fluid. This sample frequency data will be used to train a machine learning model with known rheological data obtained from an off-line rheometer. The trained prediction model will then be used to predict rheology values for an unknown fluid.

1.2 AIMS & OBJECTIVES

This project aims to investigate the development of a real-time cyber physical system that uses the concepts of Internet of Things and Big Data Analytics in Industry 4.0 to monitor rheological properties of a fluid in a continuous manufacturing process. The project also aims to extend the process developed from a monitoring system to a measuring system by applying Artificial Intelligence tools to predict unknown properties.

At the end of this project, the following objectives are expected to have been achieved:

- ✓ Develop a pilot or experimental setup that mimics a continuous manufacturing process;

- ✓ Investigate the use of a passive acoustic emission sensor to detect acoustic waves generated by the fluid in a continuous flow within the experimental setup;
- ✓ Investigate the quality of acoustic signal waves detected by the passive acoustic emission sensor;
- ✓ Investigate the sensitivity and tolerance limits of the acoustic signals generated for different fluid types and at different process conditions;
- ✓ Process acoustic signal waves into frequency spectra and eventually a Rheological Fingerprint that provides visual monitoring of changes in rheology;
- ✓ Development of a supervised machine learning model that can calculate by inference, the rheological values of "unknown" fluids in process.

1.3 THESIS STRUCTURE

The content of this project thesis has been compiled in the following order:

- Chapter Two presents the concepts of Newtonian and Non-Newtonian Rheology, its definitions and mathematical models used to characterise the different types of fluids. It shows the mathematical relationships between the core rheological values that are to be studied in this research, namely stress, shear rate and viscosity and how the three major rheological models can be related to one another which is important to the development of a machine learning model later on in this research work. Next, the chapter introduces the different techniques used widely in industry to measure rheology, highlighting the pros and cons of each technique and introduces the concept of Passive Acoustic Emission (PAE) and how that concept has been applied as a non-invasive, alternative technique in process flow monitoring. The concept behind Machine Learning and how artificially intelligent systems can be developed from machine learning algorithms is then introduced and finally, how the concepts of passive acoustic emission sensing and machine learning have been combined to develop a cyber physical device that is able to measure rheology as an alternative to conventional techniques currently used in industry.
- Chapter Three presents the experimental devices used to carry out this research; a conventional offline rheometer widely used in industry and an experimental rig built to mimic a continuous manufacturing process with the passive acoustic sensor placed on-line. The offline rheometer will be used to collect rheological data that will serve as reference values for the machine learning model later developed. Chapter Three also introduces the fluids of choice and why they have been chosen for this research, the methods by which research data will be collected on both the offline rheometer and the experimental rig, and the methods by which the data collected will be processed into frequency spectra data, Rheality™ Rheological Factor (RRF™) data and finally developed into a machine learning model function.
- Chapter Four presents the results obtained from the offline rheometer, showing the relationships between stress, shear rate and viscosity as earlier discussed in Chapter Two. Chapter Four also presents results and discussion of results obtained from the passive acoustic sensor on the experimental rig, showing proof of the quality and sensitivity of the acoustic signal data generated by each sample fluid when it was run under different process conditions. The results shown in Chapter Four also provide insight into the development of various machine learning model functions to infer rheological measurements and the efficiency of these models.

- Chapter Five then closes out this research thesis with the conclusion of work done and any future work to be considered.

2 THEORY

2.1 NEWTONIAN & NON-NEWTONIAN RHEOLOGY

Newton's law of motion states that an object would remain in a constant state of rest or in constant motion except acted upon by an external force. This external force must be greater than the frictional forces that keep the object at rest (George & Qureshi, 2013). For liquids, the measure of the limiting force or frictional force to be overcome in order to move the liquid can be described as the liquid's resistance to flow or Viscosity (Malkin & Isayev, 2012).

Newton's law of viscosity states that at a given temperature and pressure, the shear stress of a fluid subjected to mechanical stress is directly proportional to its shear strain and the relationship constant is defined as the fluid's viscosity. Fluids that obey Newton's law of resistance to flow are termed Newtonian fluids where viscosity is constant regardless of shear rate. (George & Qureshi, 2013)

$$\tau = \eta \frac{\delta u}{\delta y} \tag{2-1}$$

where τ is shear stress, η is dynamic viscosity and $\dot{\gamma} = \frac{\delta u}{\delta y}$ is the rate of shear deformation/strain

$$\tau = \eta \dot{\gamma} \tag{2-2}$$

While Newton's law of viscosity represents resistance to flow or deformation of purely viscous liquids, Hooke's law uses the same principle to represent elastic behaviour in solids and both laws define the boundary for the rheology or flow behaviour of fluids as some fluids exhibit both viscous and elastic behaviour. Such fluids are termed viscoelastic fluids. For Non-Newtonian fluids, viscosity changes in a non-linear relationship with shear rate at a given temperature and pressure and its flow behaviour is typically characterised by a flow curve that would generally have three distinct regions; low shear Newtonian region, shear thinning or Power law region (as shear rate increases in this region, viscosity decreases), and high shear Newtonian region. (George & Qureshi, 2013)

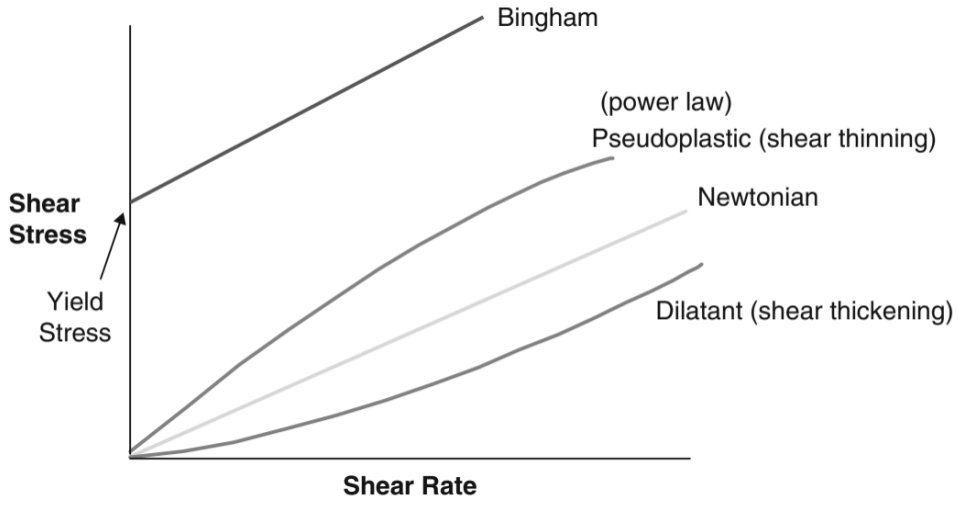

Figure 2-1: Types of rheological models (George & Qureshi, 2013)

Figure 2-1 shows the relationship between shear stress and shear strain for different rheological models. The relationship between shear stress and shear strain for Non-Newtonian fluids has been developed into many models but the most common model is the Power Law model:

$$\tau = k\dot{\gamma}^n \tag{2-3}$$

$$\mu = k\dot{\gamma}^{n-1} \tag{2-4}$$

where k is consistency index, n is the flow index defining how viscosity changes with shear rate. For $n = 1$, viscosity does not change with shear rate and viscosity equals consistency index (Newtonian fluid); $n < 1$, viscosity decreases as shear rate increases (shear thinning); $n > 1$, viscosity increases as shear rate increases (shear thickening). Some fluids also present a yield stress which is the minimum stress required to initiate flow (Wang & Chung, 2013). Fluids that exhibit Newtonian behaviour once this yield stress has been overcome are characterised by the Bingham model:

$$\tau = \tau_0 + k\dot{\gamma} \tag{2-5}$$

while fluids that exhibit Non-Newtonian shear thinning behaviour after yield stress has been overcome are characterised by the Herschel-Bulkley model:

$$\tau = \tau_0 + k\dot{\gamma}^n \tag{2-6}$$

where τ_0 is yield stress

Equation to calculate the shear rate of the fluid flowing through the pipe is given by (Darby, 2001):

$$\dot{\gamma} = \frac{4Q}{\pi r^3} \tag{2-7}$$

where Q is the volumetric flowrate of the fluid and r is the radius of the pipe.

2.2 TECHNIQUES USED IN MEASURING FLUID RHEOLOGY

A viscometer is a device that measures viscosity by applying force to a liquid on a surface and measuring the corresponding effect the force has on the liquid where the applied force is converted mathematically to shear stress and the corresponding effect on the liquid or the rate of displacement of the liquid is converted to shear rate (Barnes, 2000) and the liquid viscosity can then be calculated using equations discussed in Section 2.1.

A rheometer is similar in principle to a viscometer in that both devices are used to measure the deformation of a fluid but while a viscometer either applies force and measures velocity or applies velocity and measures force, a rheometer applies either a stress or strain-controlled approach or an extensional stress or strain approach (Macosko, 1996) to measuring more complex rheological properties. Rheometers can be split into two classes (Macosko, 1996) of either drag flow or pressure-driven flow based on their core principle of generating controlled shear. Drag flow rheometers generate shear between a fixed and moving solid surface while Pressure-driven flow rheometers generate shear by pressure difference over a closed channel (Macosko, 1996). Types of drag flow rheometers include the sliding plate, concentric cylinder, cone and plate and parallel disk rheometers while types of pressure-driven flow rheometers

include the capillary flow, slit flow and axial annulus flow rheometers. Extensional rheometers are used for materials that would resist deformation.

In the Cosmetics and Personal Care industry, rheology monitoring is fundamental to the development of formulation, process design and quality control in manufacturing needed to remain competitive in the industry. Basic consumer qualitative benchmarks such as look and feel of the product on initial application and after application rely heavily on the rheology of the product, this is besides the effect that the product's rheology has on its production, packaging and storage. Rheology measuring and monitoring becomes useful for reviewing and monitoring the effects of formulation changes, storage or mixing time changes as well as temperature changes on the quality of the final product. It is also useful for monitoring the stability of raw materials before use in production as well as testing the quality of the final product.

For personal care products such as hair gel, the yield stress is extremely important to measure besides viscosity as this has a key impact on consumer quality evaluation of the final product, e.g. a tub of hair gel with high yield stress is perceived by consumers as having more volume. To measure or monitor the rheology of the hair gel in production, a rotational rheometer can be used in a stress-controlled test (Tzaneva, et al., 2017) to produce flow and viscosity curves which can be fitted with mathematical models such as the Herschel-Bulkley model to determine the yield stress of the sample. The cone and plate rheometer is probably the most popular rotational rheometer in use. A sliding plate rheometer could also be used to run an amplitude sweep of the hair gel sample. For products like nail polish, the final products' ability to recover after experiencing shear becomes important as a consumer quality index, e.g. the polish has to be thick enough to stick to the application brush and thin enough to transfer from brush to nail surface as well as flow enough to not leave behind brush streaks after application and dry as quickly as possible after application (Jimenez, Martínez Narváez, Xu, Bacchia, & Sharma, 2021). The rheological property that allows this to happen is called thixotropy which is a time-dependent viscosity behaviour. A thixotropic material under constant shear, temperature and pressure will experience reduction in viscosity over time. This thixotropic behaviour can be measured using a rotational or oscillatory rheometer. For products such as cosmetic or pharmaceutical creams and lotions, the feel of the product and its long-term stability are important consumer quality indices. Creams and lotions are typically emulsion products made up of normally immiscible ingredients and a change in ingredient can affect the final feel and stability of the end product. The manufacturing process could also affect the final product quality so monitoring the rheology during production is key to top quality final products (Kwak, Ahn, & Song, 2015). An oscillatory rheometer can be used to test the stability of the product by applying a sample of the product between two sliding plates, one fixed and the other mobile, keeping the frequency fixed and varying the amplitude to provide information on yield point and viscoelastic characteristics of the product. For products such as toothpaste, which is a polymer, rheology can be a lot more complex as polymers tend to have unusual rheological behaviours such as thixotropy or even extensional viscosity (Ahuja & Potanin, 2018). Extensional viscosity is the material's resistance to extensional stress (Barnes, 2000), or in simpler words, it is the materials resistance to being pulled apart. Rheological properties such as rigidity and yield can be measured using oscillatory stress sweeps on a rotational rheometer.

All use cases mentioned above involve direct application of the fluid sample on the rheometer and in most cases, these rheometer measurements happen offline, i.e. a sample is collected from

the manufacturing process at various stages and taken to a laboratory for measurement. This means the measured rheological values are never real-time without shutting down production. Advances have been made in the development of an in-line or on-line rheometer, each with its own advantages and drawbacks. Amongst a variety of research work towards the advancement of the rheometer, Chryss, Monch and Constanti-Carey of CSIRO Mineral Resources, Australia, presented their work on the development of an online rheometer for measuring suspension rheology in mineral processing on the basis of a capillary viscometer (Chryss, Monch, & Constanti-Carey, 2019). The online rheometer worked on the principle of pressure drop across a pipe of known dimensions that has been installed on a sampling point. The drawback with this online rheometer is that the pipe dimensions have to first be determined suitable for the fluid in process before deployment which means that once deployed, it is only useful for the specific fluid it was designed for, i.e. flexibility of operation is extremely limited. Liu, Zhang and team presented their work on the investigation of four types of real-time rheology measurement technologies, namely an online, rotational Couette viscometer, a pipe viscometer, a Marsh funnel which uses mathematical and physics-based algorithms, and a tuning fork technology to continuously monitor drilling fluid (Liu, Zhang, Gao, Hu, & Duan, 2021). Tronci and team presented their work on the development of a non-invasive, online rheometer that uses ultrasound sensors coupled with a physics-based theory of acoustic signal propagation and liquid velocity, and machine learning to monitor the rheology of a liquid detergent manufacturing process (Tronci, et al., 2019). This is a more flexible rheometer as the device is placed on the pipe walls and no adjustment to the setup is needed as fluid in process changes, however, because the online rheometer is driven by machine learning algorithms that are trained and validated with fluid data, extensive data processing would be required. Machin and Wei presented their work on the development of a non-invasive, online rheometer using micro electrical tomography sensors to measure velocity profiles within the pipe and using mathematical models and machine learning algorithms to calculate rheological values (Machin, Wei, Greenwood, & Simmons, 2018). Different principles and methods have been investigated in the advancement of rheology measurement and it is clear that industry is moving towards non-invasive, real time monitoring and measurement of rheology in process.

2.3 PASSIVE ACOUSTIC EMISSION FOR NON-INVASIVE PROCESS MONITORING

Acoustic Emission (AE) is the study of elastic stress waves that are produced by energy spontaneously and rapidly released from a crack or fracture in a material caused by an event. This event could be triggered by temperature, pressure fluctuations or load. AE waves are usually detected in frequency ranges between 1 kHz and 1 MHz by a MEMS accelerometer (micro electro mechanical system). The MEMS accelerometer is a piezo electric sensor which picks up these stress waves as surface displacements and converts them into an electrical signal for processing. (Rasras, Elfadel, & Ngo, 2019)

Acoustic Emission sensing is of two different types; active acoustic emission and passive acoustic emission. Active Acoustic Emission sensing mimics a feedback system in the sense that acoustic signal is fed into the process and the resulting response after the signal hits the material is detected and recorded by the MEMS sensor. Passive Acoustic Emission sensing

mimics a listening system in the sense that the sensor only picks up elastic waves generated by the movement of the material.

The theory of Acoustic Emission sensing works based on the following principles (Boyd & Varley, 2001):

$$C = \lambda f \tag{2-8}$$

where C is the acoustic velocity, λ is the wavelength and f is the frequency.

The acoustic velocity is determined by the elasticity modulus and density of the material. Solids and liquids have different measures of modulus with Young modulus (Y) describing solids and Adiabatic Bulk modulus (B) describing liquids.

$$C_{solid} = \sqrt{\frac{Y}{\rho}} \tag{2-9}$$

$$C_{liquid} = \sqrt{\frac{B}{\rho}} \tag{2-10}$$

Signal amplitude (A) and acoustic intensity (I) are defined by the following relationships:

$$A \propto \frac{1}{r} \tag{2-11}$$

$$I \propto A^2 \propto \frac{1}{r^2} \tag{2-12}$$

where r is the radial spread.

The MEMS accelerometer produces an output voltage based on the wave signals that hit the surface of the sensor and this data is captured in a time domain. The fluctuation of this output voltage over time is termed the Energy density of the output signal and it is calculated using the Root Mean Square (RMS) of the time domain:

$$RMS = \sqrt{\frac{1}{t_2 - t_1}\int_{t_1}^{t_2} V(t)^2 dt} \tag{2-13}$$

This time domain data is then converted to a frequency domain by applying Fast Fourier Transform; where x_n is the input signal data in time domain, f_k is the frequency spectrum and N is the size of the domain or number of samples in the data set:

$$f_k = \sum_{n=0}^{\mathrm{N}-1} x_n e^{\frac{-2\pi i}{\mathrm{N}}.kn} \tag{2-14}$$

Acoustic Emission (AE) monitoring by nature is a non-destructive test method and is widely used across many industries. Hou, Hunt and Williams presented their findings on the use of a non-invasive passive acoustic sensor to monitor the flow and other process parameters of silica slurry. They noted that the non-invasive passive acoustic monitoring of flow provided an advantage over commercially available flowmeters by being able to operate irrespective of the properties of the fluid in process. They found out that the signals recorded by the passive

acoustic sensor were sensitive to both solid concentration and flowrate changes (Hou, Hunt, & Williams, 1999).

Khulief, Khalifa and team presented their findings on the use of acoustic emission to detect leaks in water pipelines by placing a hydrophone inside the pipe to record signals generated by the movement of the water flow (Khulief, Khalifa, Ben Mansour, & Habib, 2012). Hefft, Antonelli and Alberini presented their findings on the use of acoustic emission in an enclosed, fully-flooded single-phase system using a recirculation flow setup and obstructing the flow with different types of obstacles. The resulting flow changes were then observed with a 2D Particle Image Velocimetry (PIV) system and Acoustic Emission (AE) signals recorded on a passive acoustic emission system to prove the viability of AE in combination with PIV to predict pipe obstructions (Hefft, Antonelli, & Alberini, 2019). They then went further to explore two and three-phase systems with the same concept (Hefft & Alberini, 2020).

The use of Acoustic Emission (AE) is widely spread among material scientists for defect detection in materials in which Merheb, Nassar and team presented findings on making use of acoustic emission to detect fouling in a plate heat exchanger (Merheb, Nassar, Nongaillard, Delaplace, & Leuliet, 2007). In flow and leak detection in the oil and gas industries, Aminu, McGlinchey and Cowell presented their work in using acoustic emission with machine learning for the monitoring of solid particles in gas pipe flow (Aminu, McGlinchey, & Cowell, 2019). In machine wear detection in mechanical industries, Li, Zhao and team presented their findings on the use of acoustic emission with a logistic regression model to monitor the operations of cutting tools and determine their operational reliability (Li, Wang, Zhao, Zhang, & Zhou, 2015).

Whitaker, Baker and team presented their findings on the application of acoustic emission on-line monitoring in powder production to determine particle size, flow and compression properties in a granulation process. Their work was based on the fact that as the granulation process progresses and particles increase/decrease in size and density, these changes would influence the compression properties of the bulk powder and hence affect acoustic emission signals to generate data that can be analysed for monitoring. (Whitaker, et al., 2000)

2.4 MACHINE LEARNING

Due to the amount of data generally associated with smart system measurements as well as the complexity in processing of the data collected by these devices, the application of Data Science tools is normally required to make sense of the process. In the case of this research work, 1,179,000 data points are recorded every second; that's 70,740,000 data points every minute and 4,244,400,000 data points every hour. Pattern recognitions, classifications and machine learning is used to infer results from the raw data obtained by the cyber physical sensors.

Data Science refers to the processes involved in generating results or output from any amount of data by recognising patterns, presenting anomalies and predicting behaviour. This is done in a systematic way by first identifying the outcome, understanding the data, extracting knowledge from the data, model, analysing and finally presenting results (Cady, 2017). Big Data refers to large amount of data collected during a process within the Internet of Things (IoT) network. Machine Learning refers to the artificial ability of mathematical models to

generate knowledge from data that is fed to it via training and validation of data sets. There are four main types of machine learning (Ayodele, 2010):

1. Supervised machine learning: This involves the use of algorithms that are fed an input or trained with a set of labelled data where the output is already known. The model learns by comparing the input data with the correct output data and discovering the errors to then modify the model accordingly. The algorithm then uses methods such as classification, regression and prediction to create and identify patterns in new unlabelled data and predict the correct output.

2. Unsupervised machine learning: Unlike with supervised machine learning, unsupervised algorithms do not have reference data to learn from but work by carrying out analysis on the data input to categorise and segregate the data based on patterns it can detect. The aim of unsupervised machine learning is to explore and put structure to data.

3. Semi-supervised machine learning: This type of machine learning works just like supervised machine learning, but learns with both labelled and unlabelled data and is used where cost is a major factor because labelled data can be quite expensive.

4. Reinforced machine learning: This type of machine learning training involves a reward system to encourage the desired output in a trial and error sequence of decisions. The goal is for the reinforcement learning agent to collect as many rewards as possible by interpreting its environment, taking actions and learning from the result of those actions. Correct actions gain a reward while incorrect actions gain a penalty.

This project makes use of supervised machine learning to establish a relational model between rheological properties of a fluid and passive acoustic emission signals generated by that fluid and prove that this model can be used to predict rheological properties of fluid on-line in a manufacturing process. With the invention of Rheality™ and the Rheality™ Rheological Factor (RRF™), Alberini, Hefft and Forte have proved a relationship between passive acoustic emission signals and rheological changes in a process flow and that acoustic emission sensing together with machine learning can be deployed to the manufacturing environment and deliver live on-line monitoring of a manufacturing process (Great Britain Patent No. WO2020260889A1, 2020).

2.5 ARTIFICIAL NEURAL NETWORK (ANN)

This section introduces the concept of Artificial Neural Network (ANN) while details of how the ANN would be applied to this research will be discussed in Chapters 3 and 4.

In Biology, the human brain is made up of billions of neurons which communicate with each other using electrical signals. Synapses allow these electrical signals to pass from one neuron to another and these synapses are located on protoplasmic projections of the nerve cell. Each neuron receives thousands of signals from other neurons that ultimately get to the cell body where a voltage response is then triggered if the cumulative signals exceed a particular threshold. This voltage response is then transmitted to other neurons through another protoplasmic projection called the axon. Figure 2-2(a) shows the essential components of a biological neuron with each neuron being made up of synapses, dendrites, cell body and axon

and a collection of neurons make up a Neural Network in the brain. Figure 2-2(b) shows the corresponding components of a biological neuron in a simple artificial neuron. Artificial Neural Network was inspired by the mechanism with which information is received and processed by the human brain.

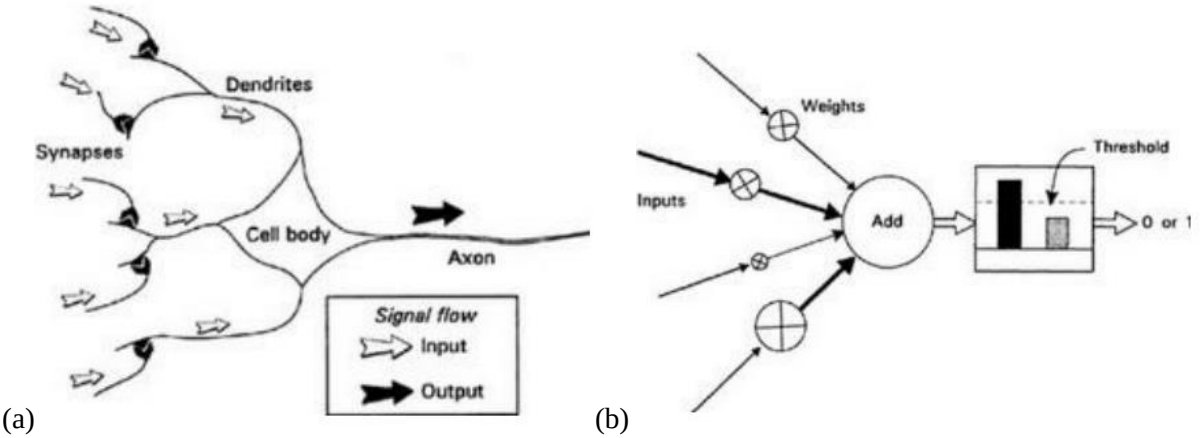

Figure 2-2: (a) Essential components of a neuron in the human brain; (b) Simple artificial neuron (Gurney, 1997)

Using the comparison in Figure 2-2, an artificial neural network by definition is a connected network of artificial neurons or nodes or units where each node is made up of artificial synapses or weights that allow for input signals to be received where each input is a number multiplied by the weight and the sum total of all weighted inputs is cumulatively collected in an artificial cell body or a node activation. If the node activation value exceeds the threshold logic unit, an output value (typically of 1) is released and if the node activation is less than the threshold, an output of 0 is released.

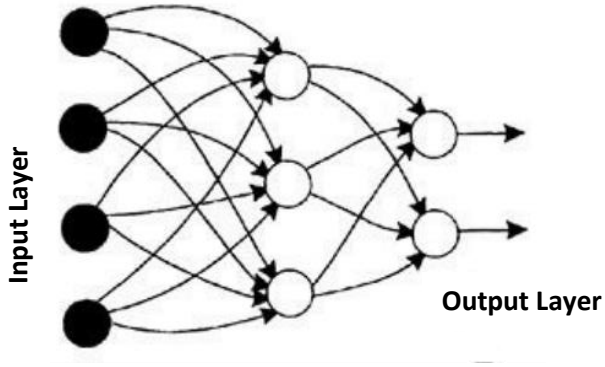

Figure 2-3: Simple example of an artificial neural network (Gurney, 1997)

Figure 2-3 shows a simple example of an artificial neural network with its input and output layers (Gurney, 1997). An Artificial Neural Network is a set of algorithms that try to recognise and map underlying relationships within a dataset on the back of the basis of operation of neurons in the human brain. Artificial Neural Network is a type of Supervised Machine Learning.

2.6 RHEALITY™ RHEOLOGICAL FACTOR (RRF™)

The Rheality™ invention is protected by the Patent Cooperation Treaty under publication number WO 2020/260889 A1. Alberini, Hefft and Forte presented their methods and apparatus used to identify rheological properties of a liquid from acoustic signals generated by the liquid's flow in a pipe. A fully flooded, recirculating flow loop was used as the experimental setup and different fluid types, ranging from Newtonian to Non-Newtonian shear thinning were used to establish the proof of the invention. An offline rheometer was used to obtain reference rheological values for the sample fluids. Each fluid sample was then circulated in the closed loop experimental setup and an acoustic sensor was used to capture acoustic signals from the fluid as it flowed through the pipe. The signals recorded per sample run was then converted into frequency spectra showing the magnitude of acoustic signal intensity as a function of frequency. Supervised machine learning algorithm was then used to distinguish and filter between useful frequency spectra and background noise (Great Britain Patent No. WO2020260889A1, 2020).

Each sample frequency spectra consists of hundreds of thousands of datapoints which was then simplified using relative variance. The relative variance of the filtered frequencies was calculated and a machine learning algorithm using principle component analysis was used to arrive at a standard frequency spectrum that represents the rheological property of the fluid and can be suitable for use in comparison and prediction of unknown fluid properties. Principle component analysis was used to split the hundreds of thousands of datapoints in the sample frequency spectrum into 10 sections with each section representing a parameter P1 to P10 as shown in Figure 2-4. To produce the results in Figure 2-4, the patent inventors made use of a continuous flow system to simulate an actual manufacturing process. The fluid mixture in the simulation was monitored using the acoustic sensor from inception up to 5 mins after high shear mixing was attained in order to track the rheological changes in the fluid over time. (Great Britain Patent No. WO2020260889A1, 2020).

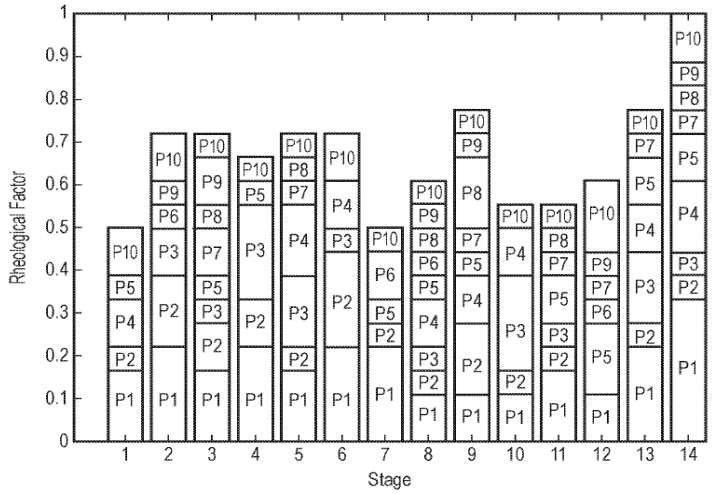

Figure 2-4: Rheality™ Rheological Factor parameters at different stages of mixing and flow in a continuous loop with stage 1 being 5 minutes into emulsification and stage 14 being after 5 minutes of high shearing (Great Britain Patent No. WO2020260889A1, 2020).

Each section or parameter is a set of stored frequencies considered to represent a rheological factor. The example frequency spectra shown in Figure 2-4 is a simulation of the process of

manufacturing a liquid product and the change in relative magnitudes of each parameter and the corresponding change in magnitude of each frequency spectrum from stage 1 to stage 14 can be used to describe the development of the liquid's rheological profile as it moves from one stage to the next with stage 1 representing after 5 minutes of emulsification and stage 14 representing after 5 minutes of high shear mixing. A combination of these parameters can then be used to determine different rheological properties of a liquid using machine learning.

The invention method can be summarised as involving the use of a sensor (Figure 2-5) attached to a rod at the pipe wall and extending into the pipe to detect acoustic signals generated by a liquid flowing through the pipe; the acoustic signal is then sampled and transformed to generate a sampled frequency spectrum which would then be correlated to a database of stored frequency spectrum of known liquids and their rheological properties to then predict and identify the rheological property of the sampled liquid based on this database.

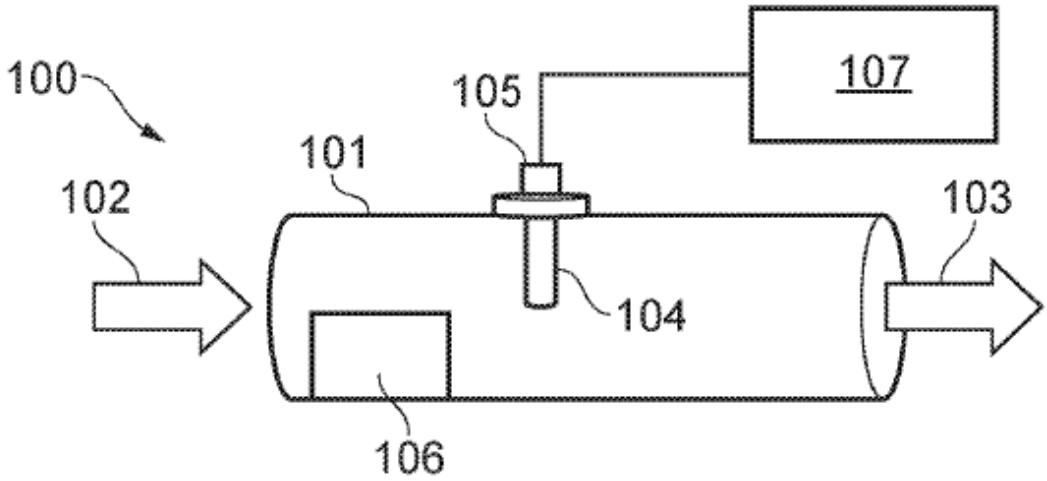

Figure 2-5: Illustration of the Rheality™ device (Great Britain Patent No. WO2020260889A1, 2020)

Figure 2-5 shows an illustration of the Rheality™ device (100). The device is made up of an acoustic sensor (105) placed on the outer wall of the process pipe (101), at the end of a pin or rod (104) that sits inside of the pipe and comes in contact with the fluid as it flows (102 & 103) through the process pipe. A piece of steel (106) can also be installed as an obstruction to the flow in order to enhance the acoustics generated by the fluid (Great Britain Patent No. WO2020260889A1, 2020).

The invention is said to be able to distinguish between Newtonian and Non-Newtonian fluid as well as distinguish between a fluid that is shear thinning or shear thickening with recorded evidence of up to 95% prediction accuracies. Depending on the robustness of the stored frequency spectrum in the reference database, it is said to be possible to also determine rheological factors such as viscosity, rate index, yield stress and consistency of a sampled fluid (Great Britain Patent No. WO2020260889A1, 2020). This research work will aim to confirm or disprove these claims.

3 MATERIALS & METHODS

3.1 EXPERIMENTAL OVERVIEW, SCHEMATICS & SETUP

This research work will be focused on gathering acoustic emission signals collected and transmitted by an acoustic emission sensor fitted on a custom experimental rig consisting of a jacketed tank and pump coupled in a closed, continuous flow loop. The acoustic signals are then amplified and recorded on an oscilloscope which can then be processed using Fast Fourier Transform (FFT) on MATLAB (MathWorks Inc, USA) to generate frequency versus intensity plots.

Rheology data will also be obtained from an Offline Rheometer, Discovery HR-1 (TA® Instruments, Inc., USA) to serve as the reference data for each sample fluid run in the experimental rig and will serve as the target rheological values for the processed signal data since the principle of operation of the passive acoustic emission monitoring of rheology is measurement by inference.

The FFT data will then be further processed using the Rheality™ Rheological Factor (RRF™) function to group the data by frequency into 10 parameters, each representing a particular property of the liquid that has been measured. The RRF™ function is a patented function provided by Rheality Ltd (Birmingham, UK) that uses patent protected algebraic steps to differentiate complex frequency ranges into simpler sequences of numbers. In this case, the RRF™ function converts the over 500,000 FFT frequency data of the raw signals into 10 parameters. The RRF™ data will be used to generate an inferred rheological value by creating a matrix of the RRF™ data processed for various fluids and process conditions, split into three sets, one for training the machine learning model, one for testing and the other for validating the model.

3.1.1 EXPERIMENTAL RIG

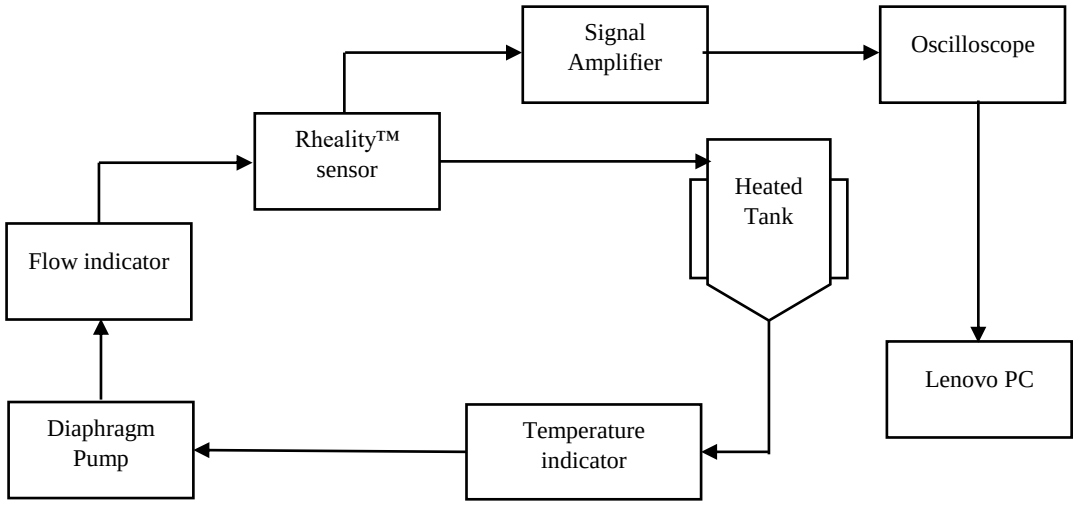

Figure 3-1: Experimental rig flowchart

Figure 3-1 shows a simple flowchart of the experimental rig setup for this research work. The experimental rig, as further illustrated in Figure 3-2, was made up of a 40 L jacketed vessel which was heated by ICS i-Temp ci90 t9.1 heat exchanger (ICS Cool Energy Ltd, UK). Various samples of fluid were recirculated by a SPX diaphragm pump model TA-15BSH-FDA (SPX

Flow Technology, Belgium) through a DN25 stainless steel pipe network of 25.4 mm diameter. The acoustic sensor (Figure 2-5) used was a Vallen 375kHz piezoelectric broadband sensor (Vallen Systeme GmbH, Germany) and it was placed on the face plate of the DN25 stainless steel probe that had been inserted and welded to the 25.4 mm diameter pipe and the flow was measured by an OG4 oval gear flowmeter (Titan Enterprise, UK) and the temperature of the fluid was measured using a Testo 905-T1 K thermometer (Testo SE & Co, UK). The sensor was encased within an IP40 rated stainless steel capsule with a 20.3mm ceramic face plate placed on the outer wall of the process pipe so does not come in direct contact with the fluid, hence non-invasive. The Vallen 375 kHz sensor was connected to a 34-dB gain preamplifier which amplifies the signals generated by the sensor. The preamplifier was powered by a DCPL2 decoupling unit and the amplified signal was then processed through a PicoScope® 5243B oscilloscope (Pico Technology Ltd, UK) connected to a Lenovo ThinkPad X1 Carbon Gen 8 personal computer (Lenovo Group, China) via a USB 2.0.

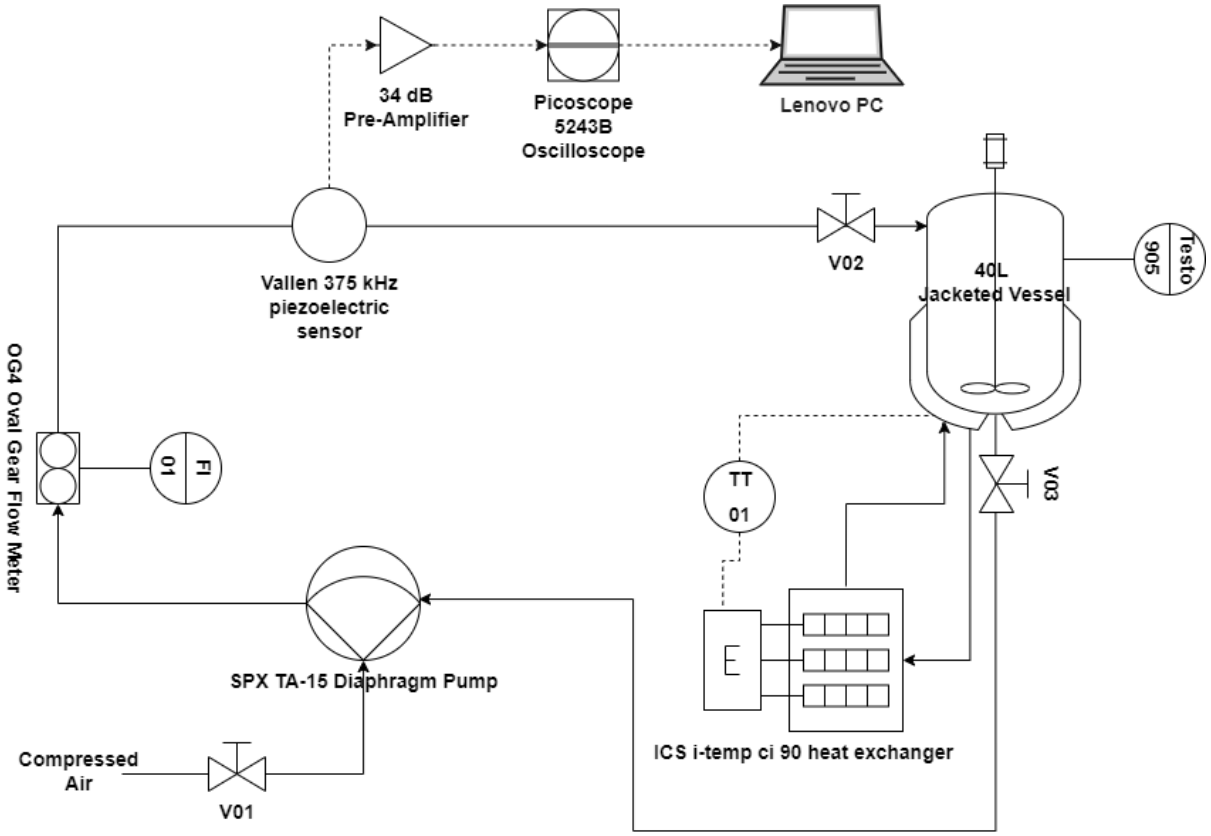

Figure 3-2: Experimental rig schematic

3.1.2 OFFLINE RHEOMETER SETUP

Offline rheological data was obtained using a controlled-stress, rotational cone and plate rheometer, Discovery HR-1 Rheometer (TA® Instruments, Inc., USA) which has a Peltier plate Steel – 108764 element for temperature control. A 60 mm 2.005° cone plate was used as the desired geometry to measure each sample rheology. Figure 3-3(a) shows an image of the rotational cone and plate rheometer used while Figure 3-3(b) is a schematic of the rheometer, showing in better detail, the cone geometry and fluid sample placement between the cone geometry and the fixed plate. The Peltier plate is connected to a water bath for temperature control and the shaft that rotates the cone geometry is driven by compressed air. Each sample run generated either a temperature ramp or a flow ramp based on the desired rheological

measurement needed and the rheological measurement data was processed with TRIOS software version 4.0.2.30774 (TA® Instruments, Inc., USA).

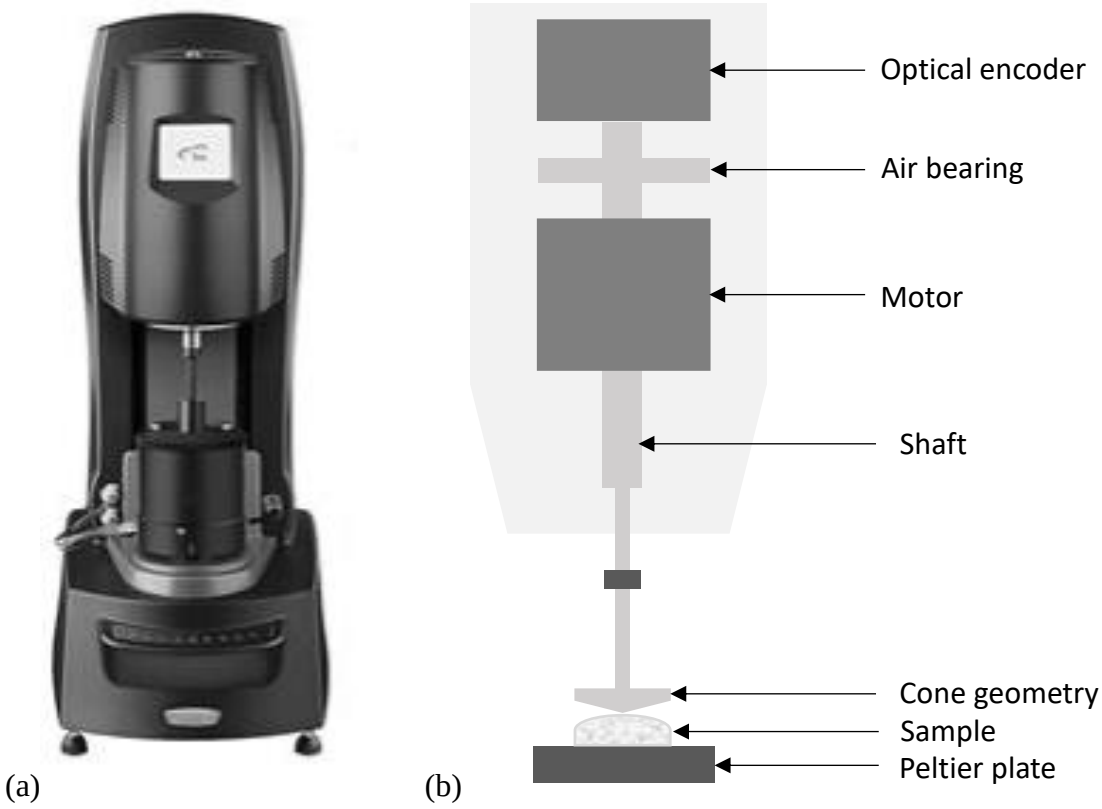

Figure 3-3: [a] Discovery HR-1 Rheometer [b] Offline Rheometer setup schematic

The rheometer applies torque and measures angular displacement and angular velocity, and uses these measurements to calculate stress, strain and strain rate. The choice of geometry also factors into the calculation of rheological values as both the stress and strain constants depend on geometry. Viscosity is calculated from calculated stress and strain values. Temperature ramp measurement on the cone and plate rotational rheometer is used to measure viscosity changes as temperature changes by maintaining a constant shear stress or shear rate and increasing the temperature of the sample fluid in steps. Flow ramp measurement is used to measure yield stress and viscosity flow curves by measuring the stress and viscosity for every step change in shear rate using a stead state algorithm. Apart from shear rate as the variable, flow ramp can also use shear stress, velocity or torque as the step variable.

3.2 MATERIAL

3.2.1 NEWTONIAN FLUID – GLYCEROL SOLUTION

Glycerol is a clear, odourless, colourless, sweet tasting viscous solution which is soluble in water, ethanol and ethyl ether. Glycerol is widely used in the food, personal care and pharmaceutical industries. CA2805 Crude Glycerol of composition 93% Glycerol (56-81-5), 4% water and 3% fatty acid (67701-06-8) strength and 92.09382 g mol^{-1} molecular weight and specific gravity of 1.257 was supplied by ReAgent (ReAgent Chemical Services Ltd) in a 200 L drum and dispensed using a manual chemical transfer steel pump. 15 L of Glycerol was

dispensed using the manual chemical transfer pump into a 10 L bucket in batches of 5 L per batch and subsequently transferred to the jacketed tank on the experimental rig (Figure 3-1). Each experimental batch of Glycerol was used at various temperatures between 20 °C and 75 °C and run at different volumetric flowrates to obtain acoustic signal data for the various process conditions. This acoustic signal data was then processed relative to the temperature and flow sweep data obtained from an offline rheometer. Glycerol is a Newtonian fluid and its shear stress is directly proportional to its shear strain so its viscosity, η is defined by the ratio of its shear stress against shear strain rate as in equation (2-1).

3.2.2 NON-NEWTONIAN FLUID – SODIUM CARBOXYMETHYL CELLULOSE SOLUTION

Solutions of Sodium Carboxymethyl Cellulose (CMC) were also used to investigate acoustic measurement of rheology. Sodium Carboxymethyl Cellulose is the sodium salt of carboxymethyl ether, a polymeric cellulose derivative that is soluble in water and forms a clear, colloidal solution. It is widely used in food, personal care, detergent, pharmaceutical industry as a rheology modifier. Sodium Carboxymethyl Cellulose of 700,000 g mol^{-1} molecular weight, pH of 6.5 to 8.5 and degree of substitution of 0.8 to 0.95 supplied by Sigma Aldrich (Sigma-Aldrich Solutions, n.d.) was used to prepare 0.5 wt.% concentration by diluting 75 g of CMC in 14.925 kg of water in a tank gently stirred for about 3 hrs at room temperature. 0.75 wt.% concentration was also prepared by diluting 112.5 g of CMC in 14.888 kg of water in a tank gently stirred for about 4 hrs at room temperature.

15 L of the 0.5 wt.% and 0.75 wt.% solutions of CMC were then circulated in the experimental rig (Figure 3-1) at temperatures between 20 °C and 55 °C and at different volumetric flowrates to obtain acoustic signal data for the various process conditions. This acoustic signal data was then processed relative to the temperature and flow sweep data obtained from an offline rheometer. The CMC solution is a non-Newtonian fluid that exhibits shear thinning rheological behaviour and its flow sweep (shear stress vs shear rate) curve was characterised using the Power Law model. As solutions of CMC do not present a yield stress, its rheological model equation is as shown in equation 2-3.

3.2.3 NON-NEWTONIAN FLUID WITH YIELD STRESS – CARBOPOL® 940 SOLUTION

Carbopol® 940 polymer is a registered trademark of Lubrizol Corporation (Wickliffe, OH, USA). It is a white, fluffy powder made from acrylic acids and soluble in water to form clear, viscous solutions or gels at controlled pH and temperature. Dissolving Carbopol in water forms an acidic polymer that can be neutralised with a base such as Sodium Hydroxide (NaOH) to form a salt. It is generally used as a rheology modifier in the personal care industry. Solutions of Carbopol were also used to investigate acoustic measurement of rheology. Carbopol supplied by Lubrizol (Lubrizol Corporation, Wickliffe, OH, USA) was used to prepare 0.1 wt.% and 0.25 wt.% concentration by 15 g of Carbopol in 14.985 kg of water in a tank gently stirred for about 3 hrs at room temperature and pellets of NaOH were used to neutralise the acidic polymer solution till a pH of 5.0 was obtained. The 0.75 wt.% concentration was also prepared by diluting 37.5 g of Carbopol in 14.625 kg of water in a tank gently stirred for about

5 hrs at room temperature and pellets of NaOH were used to neutralise the acidic polymer solution till a pH of 5.0 was obtained.

15 L of the 0.1 wt.% and 0.25 wt.% solutions of Carbopol were then circulated in the experimental rig (Figure 3-1) at temperatures between 20 °C and 55 °C and at different volumetric flowrates to obtain acoustic signal data for the various process conditions. This acoustic signal data was then processed relative to the temperature and flow sweep data obtained from an offline rheometer. The Carbopol solution is a non-Newtonian fluid that exhibits shear thinning rheological behaviour but also presents a yield stress, hence its rheological curve (shear stress vs shear rate) is characterised by the Herschel-Bulkley equation as shown in equation 2-6.

3.3 METHOD

3.3.1 OFFLINE RHEOLOGY DATA COLLECTION

To start each run, the compressed air line was switched on, the rheometer was powered on and the water bath was switched on. The computer was then switched on and the TRIOS (TA® Instruments, Inc., USA) software was loaded and connected to the rheometer. The 60 mm 2.005° cone was inserted and auto-calibrated by the TRIOS software. Samples of the Glycerol solution that had been circulated in the experimental rig (Figure 3-2) were collected into 10ml chemical sample test tubes. These samples were then dispensed using a plastic pipette onto the Peltier plate of the rheometer (Figure 3-3).

Experiment type was setup on the TRIOS software to execute either Temperature Ramps or Flow Sweeps on the sample dispensed on the Peltier plate. For Temperature ramp experiments, the start temperature and end temperature were set at 25 °C and 75 °C, being the minimum and maximum temperature planned for sample experimental runs on the experimental rig (Figure 3-1). The ramp rate set at 5 °C and the shear rate was calculated by applying equation 2-7 on the flow rate data collected by the oval gear flow meter and using the pipe radius data from the experimental rig (Figure 3-2). For Flow sweep experiments, the shear rate range was set to the minimum and maximum shear rates equivalent to the planned flow rates for sample runs on the experimental rig (Figure 3-1). Each experiment on the offline rheometer was controlled by the TRIOS software and the resulting data was automatically collected and plotted by the TRIOS software. Each result plot was then analysed on the TRIOS software using specific best fit plots of stress vs strain data; a Newtonian plot for the Newtonian fluid, a Power Law plot fit for the Non-Newtonian fluid and a Herschel-Bulkley plot fit for the Non-Newtonian fluid with yield stress. This experimental method was run in triplicates and repeated for all the sample materials of choice (Sodium Carboxymethyl cellulose and Carbopol solutions) using planned temperature and flow rate ranges as the minimum and maximum parameter values.

3.3.2 EVOLUTION OF THE EXPERIMENTAL RIG

In order to model a continuous process flow as would be seen in the manufacture of liquid products such as hand gel which would normally involve batch mixing of ingredients and pumping the mixture through a piping network over to packaging, the experimental rig (Figure 3-1) was fabricated to include a 40L jacketed vessel connected to a diaphragm pump by a network of 2.54 mm diameter steel pipes which runs in a continuous loop from the bottom of

the vessel and returns to the top of the vessel. A jacketed vessel was chosen in order to be able to simulate multiple temperature conditions on the rig. A diaphragm pump and a gear flow meter were fitted on the rig because of their ability to handle viscous fluid.

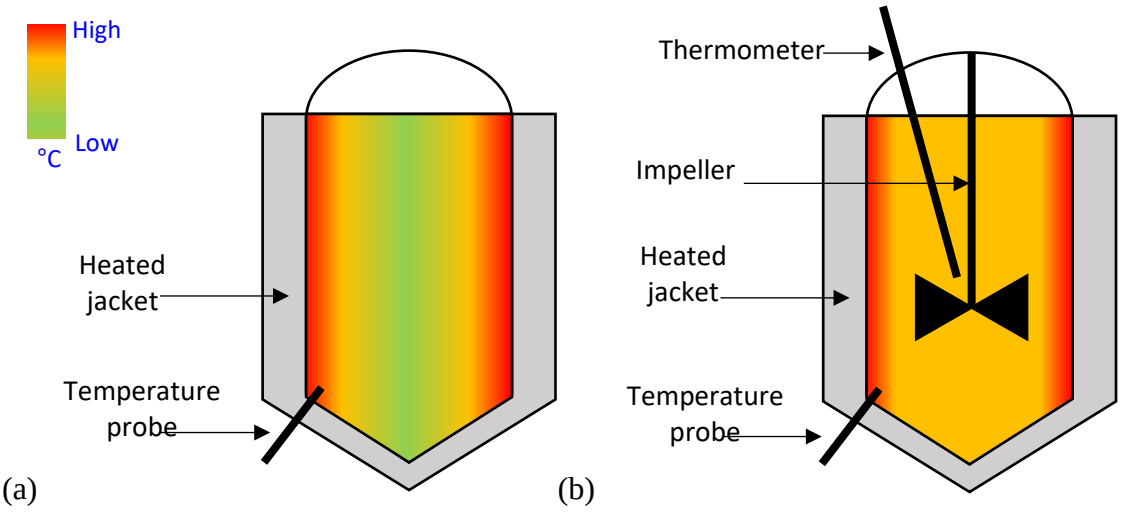

Figure 3-4: Schematic of 40 L jacketed vessel showing temperature gradient of fluid inside the vessel with (a) showing before and (b) showing after introduction of impeller and thermometer

The jacket of the vessel was fitted with a temperature sensor that provided temperature data of the heating jacket as feedback to the heat exchanger connected to regulate temperature of the vessel. It was however, discovered that the sensor was not giving a true reading of the fluid temperature because the fluid in the vessel was not being evenly heated by the jacket with fluid at the walls being at a higher temperature than fluid at the centre of the vessel. In order to correct this, an impeller was introduced to the vessel as shown in Figure 3-4 to aid in even mixing and heating of the fluid in the vessel. Figure 3-4(a) shows a schematic of the temperature gradient within the 40 L jacketed vessel before the introduction of the impeller while Figure 3-4(b) shows the better distributed temperature gradient in the vessel after the introduction of the impeller. A thermometer was also introduced to read fluid temperature from different points within the vessel to ensure adequate mixing and heating was taking place.

3.3.3 ONLINE RHEOLOGY DATA COLLECTION

To start each run on the rig, the compressed air line was switched on and the Rheality™ device (Figure 2-5) was installed on the rig (Figure 3-1). 15 L of the fluid of choice was then dispensed into the jacketed tank and the temperature of the fluid in the tank was taken. The heat exchanger was then activated to get the fluid in the tank to the desired temperature. The diaphragm pump was switched on to begin fluid circulation within the rig. The compressed air pressure was adjusted to reach the desired fluid flow rate and once the desired temperature and flow rate was achieved, the recording of the acoustic signal readings commenced. The flow rate of each experimental run was then converted to its corresponding shear rate by applying equation (2-7).

For each sample data capture, the number of samples (N in equation 2-14) was set to 600,000 to ensure the sampling frequency is double the resonance frequency of the sensor and the

hardware resolution was set at 16 bits. A collection time of 50 ms/division was chosen as the time required to collect stable spectra and an amplitude range of ± 200 mV. Other data capture parameters used in the oscilloscope software, PicoScope 6 5243B (Pico Technology Ltd, UK) include a sample interval of 848 ns, sample rates of 1.179 MS/s and a total of 100 buffers.

The PicoScope data was collected in triplicate and saved as [.psdata] and [.mat] files. The same procedure was then repeated for the sample fluids and process conditions listed in Table 3-1. Temperature data in Table 3-1 was obtained using the Testo thermometer and the Shear rate data was calculated using flow rate data obtained from the oval gear flowmeter and employing equation 2-7 to convert the flow rate to shear rate.

Material of Choice	**Temperature [°C]**	**Shear rate [s^{-1}]**
Glycerol	20	20.7
Glycerol	21	20.7
Glycerol	21	29.5
Glycerol	30	20.7
Glycerol	30	29.5
Glycerol	35	20.7
Glycerol	35	29.5
Glycerol	35	38.8
Glycerol	40	20.7
Glycerol	40	29.5
Glycerol	44	20.7
Glycerol	50	20.7
Glycerol	50	29.5
Glycerol	50	38.8
Glycerol	50	49.2
CMC 0.50 wt.%	24	38.8
CMC 0.50 wt.%	24	46.6
CMC 0.50 wt.%	24	53.1
CMC 0.50 wt.%	35	38.8
CMC 0.50 wt.%	35	46.6
CMC 0.50 wt.%	35	53.1
CMC 0.50 wt.%	50	46.6
CMC 0.50 wt.%	50	53.1
CMC 0.75 wt.%	32	38.8
CMC 0.75 wt.%	32	46.6
CMC 0.75 wt.%	35	46.6
CMC 0.75 wt.%	40	46.6
CMC 0.75 wt.%	46	46.6
CMC 0.75 wt.%	50	46.6
Carbopol 0.10 wt.%	21	40.6
Carbopol 0.10 wt.%	21	46.6
Carbopol 0.10 wt.%	21	53.1
Carbopol 0.10 wt.%	35	46.6
Carbopol 0.10 wt.%	45	46.6
Carbopol 0.10 wt.%	50	46.6
Carbopol 0.25 wt.%	29	40.6

Material of Choice	Temperature [°C]	Shear rate [s^{-1}]
Carbopol 0.25 wt.%	29	46.6
Carbopol 0.25 wt.%	29	53.1
Carbopol 0.25 wt.%	45	46.6
Carbopol 0.25 wt.%	51	46.6

Table 3-1: Fluid properties for each experimental run on the rig

3.3.4 ACOUSTIC DATA PROCESSING (RRF™) USING RHEALITY GAMMA FUNCTION

Each set of .mat files were processed with MATLAB R2020a (MathWorks Inc, USA) using the Fast Fourier Transform function first to convert the time domain signals to a frequency domain based on equation (2-14). The frequency domain data (FFT) generated has over 500,000 data points and this FFT data is simplified using the Rheality™ Gamma function. The frequency domain data can be plotted as an amplitude versus frequency plot on a logarithmic scale to show frequencies of interest as shown in Figure 3-5. The frequency domain data contains signals generated by the fluid as well as background and irrelevant noise that needs to be filtered out. The Rheality™ Gamma function deducts the background and irrelevant frequency data from the sample frequency spectrum and using principal component analysis, transforms the over 500,000 data points into 10 parameters that define unique rheological qualities of the sample fluid. Figure 3-6 shows the instantaneous measurement of 100 buffers of acoustic signal data for a sample of Glycerol flowing through the experimental rig. Each instantaneous measurement or individual buffer contains the over 500,000 data points which become 10 RRF™ parameters and the sum total of all 10 parameters equals the signal intensity at that moment of capture. The principle of operation of the RRF™ function is protected by patent WO/2020/260889 A1 (Great Britain Patent No. WO2020260889A1, 2020).

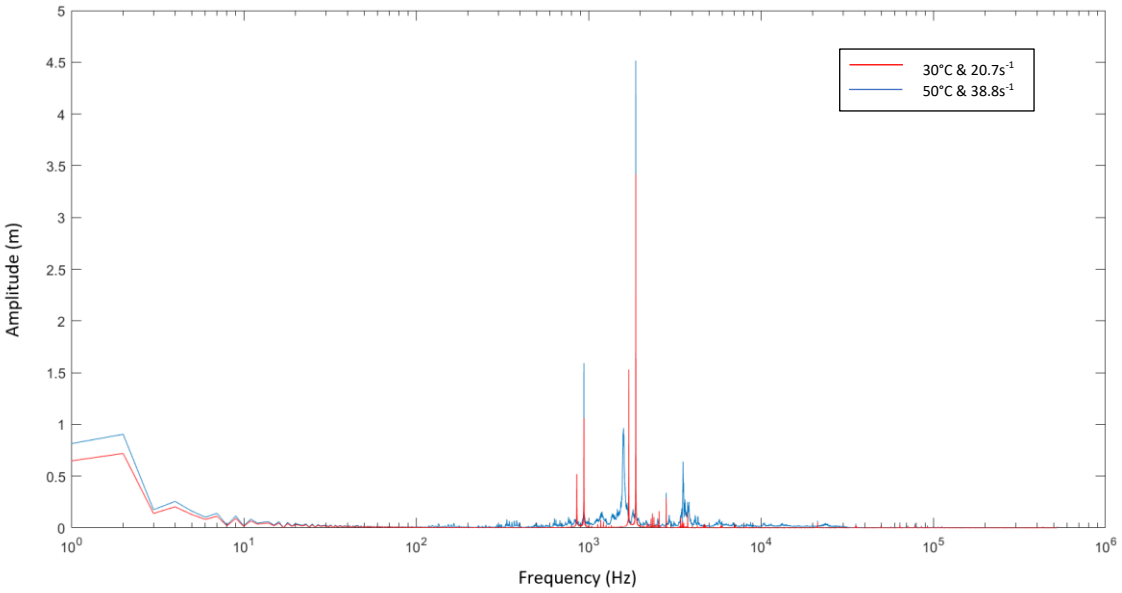

Figure 3-5: Example of Fast Fourier Transform plot of frequency domain data showing frequencies of interest for a solution of Glycerol at two different conditions.

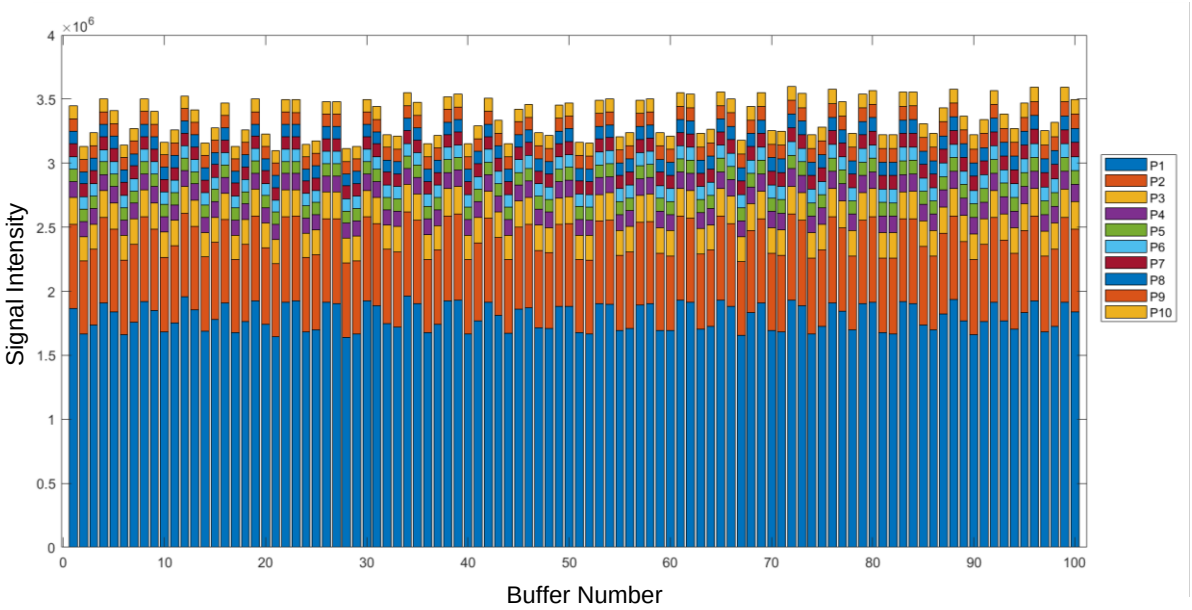

Figure 3-6: Instantaneous measurement of acoustic signals on a sample of Glycerol running through the experimental rig for a 100-buffer size reading showing the 10 RRF™ parameters for its individual sample frequency spectrum

For each sample condition as outlined in Table 3-1, 100 buffers of acoustic signal recording was captured in triplicates and stored in the format, T[temperature]flow[shear rate]_[run number], e.g. T20flowA_2 being the second run for sample fluid at 20 °C and the flow rate corresponding to shear rate 20.7 s^{-1}. The average of the 100 instantaneous buffers is then used to represent the rheological fingerprint for that sample fluid at the conditions recorded.

3.3.5 ESTABLISHING STEADY STATE ACOUSTIC SIGNALS

Once it was established that all required parameter data such as flow rate from the oval gear flow meter, fluid temperature from the Testo thermometer, could be obtained successfully from the experimental rig (Figure 3-2), it was necessary to now establish steady state conditions from the acoustic emission sensor. Data required to establish steady state conditions were collected by running a sample of Glycerol solution through the experimental rig using the method described in Section 3.3.3. Experimental parameters for the signal data collected are as outlined in Section 3.3.3 with the exception of the value for total number of buffers. For the first experimental run, the total number of buffers was set at 1 buffer and acoustic signal data was collected and recorded. For the next experimental run, buffer size was increased to 2 and the process of collecting acoustic signal on the experimental rig was repeated, signal data recorded and saved. This was repeated with increasing buffer size of 3, 4, 5 up to 100 buffers to determine the minimum number of buffers required to collect well developed signals. The set of signal data collected at these buffer sizes were then analysed using methods described in Section 3.3.4 to generate the RRF™ values for each set of experimental runs.

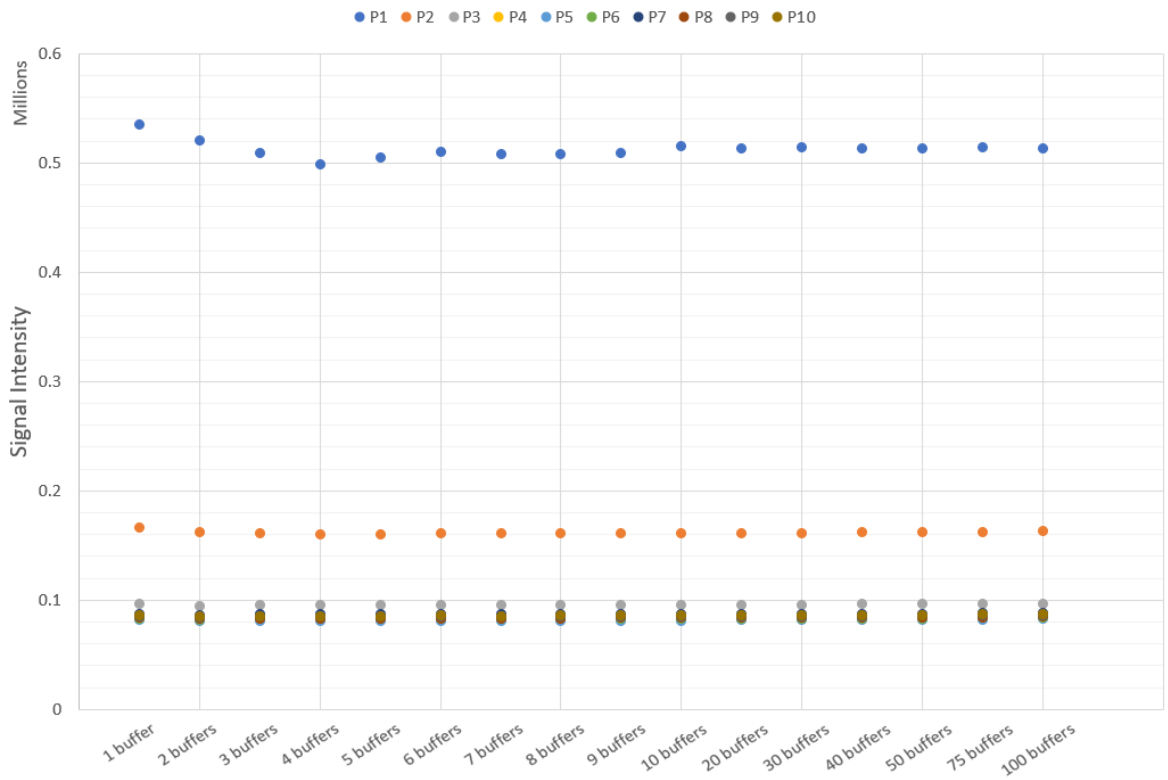

Figure 3-7: Scatter plot showing individual RRF™ parameter values for a sample of Glycerol solution at different buffer sizes to establish minimum buffer required for stable acoustic data

A single buffer is recorded in 0.5s and as can be seen in Figure 3-7, the averaged signal intensity per buffer size starts to level out for buffer sizes greater than 10. This means that after 5s from inception of signal recording, the acoustic signal becomes steady for the duration of the recording and any 10 or more buffers can be averaged to give a true representation of the acoustic fingerprint for the fluid being sampled. For the rest of the research investigation, a buffer size of 100 was chosen.

3.3.6 BACKGROUND NOISE ANALYSIS

In acoustic monitoring, it is important to ascertain the quality of the acoustic signals being recorded by recognising and providing a factor to cater to background noises present in the environment in which the acoustic system is being used. Sounds and vibrations being generated by other equipment in the environment or noise generated from people or equipment in motion can alter the quality of the acoustic signal being recorded. In mitigating the effect of background noise, the configuration of the acoustic sensor in use comes to play. The acoustic sensor measures surface displacement caused by stress waves generated and in placing the sensor with its membrane face down, directly on the pipe obstruction that generates the required stress wave helps in reducing the effect of background noise. But because background noise cannot be totally eliminated, the RRF™ function makes provision for a base reading that is meant to be the acoustic signal reading when there is no flow in the pipe and the entire system is not running.

To record the baseline background noise, acoustic signal data was collected with the Rheality™ device in place on the rig (Figure 3-2) before the diaphragm pump was switched on and before

flow circulation within the closed loop to record any extra noise that might be picked up during sample runs. A plot of the amplitude versus frequency data with the frequency data axis being plotted in logarithm (Figure 3-8) shows the signal amplitude peaks at frequencies of interest. Figure 3-8 shows a comparison of the amplitude-frequency plot of background noise and a random sample flow measurement, emphasizing the need to account for background or irrelevant noise in the processing of the rheology acoustic signal.

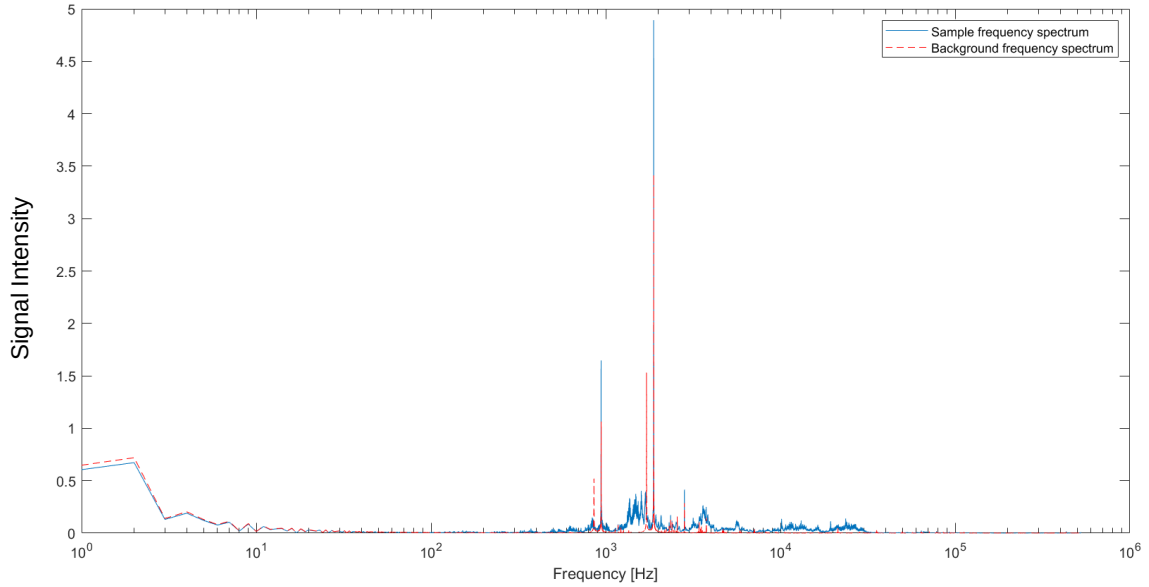

Figure 3-8: Plot of Fast Fourier Transformed signals for background noise and sample flow measurement for Glycerol sample running in the experimental rig

3.3.7 DATA ANALYSIS FOR SUPERVISED MACHINE LEARNING

The data required for training the supervised model is an input and output matrix as shown in Figure 3-9. Figure 3-9 shows the Artificial Neural Network used in training and validating the machine learning model function for predicting rheological values, showing the 10 input values, the hidden layer which contains nodes that carry out the complex modelling of the training dataset, the output layer which contains nodes that produce the final output results and the output value. The input matrix is the set of 10 rheological parameters for the sample fluid that was created using the Rheality Gamma function to process acoustic signal data collected at different temperatures and constant flow rate such that each matrix contains RRF™ data for a sample fluid collected at a fixed shear rate and multiple temperatures. The input and output data set is then split into three; 70% for training the model, 15% for testing and 15% for validation of the model. The Levenberg-Marquardt backpropagation algorithm was used to train the model by minimizing a function (y) to find its lowest point. This is done by calculating an approximation to the function (y) at a particular iteration point (x(n)), approximating the next iteration point (x(n+1)) and then comparing the result of the approximation to the actual function to determine how accurate the approximation is at the next iteration. If the approximation is not good enough, the algorithm adjusts itself.

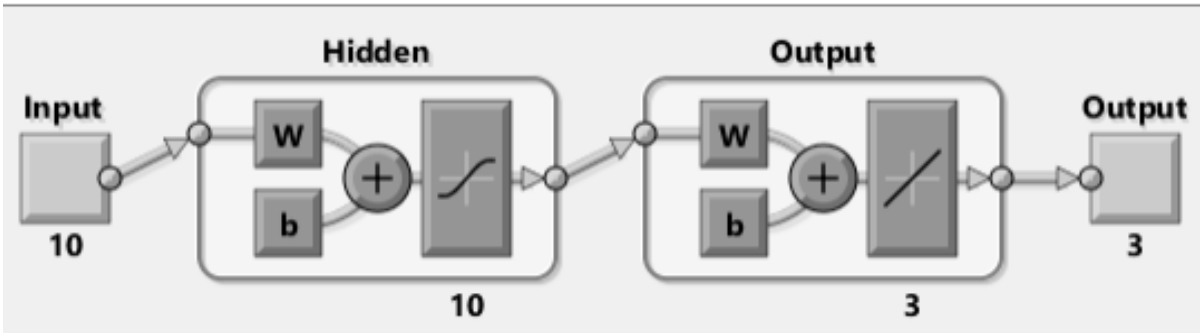

Figure 3-9: Artificial Neural Network for processing online rheology data showing 10 input values and 3 output values and the makeup of the neural network

To obtain the input matrix data, the .mat file of acoustic signal recording per experimental run containing 100 buffers was imported into MATLAB R2020a and each individual buffer was converted from its time domain to its frequency domain using equation (2-14). Each buffer contained 589,623 data points in its time domain and the corresponding frequency domain generated 524,289 data points after performing a Fast Fourier Transform of the 589,623 data points, creating a *524,289×100* FFT data matrix for all 100 buffers in a single experimental run. The Rheality™ Gamma function was then used to transform this *524,289×100* FFT data matrix into a *10×100* RRF™ matrix after deducting background and irrelevant signals from the FFT data matrix. The Rheality™ Gamma function uses the principle of principal component analysis as explained in Section 2.6 to classify the 524,289 data points in each buffer into 10 parameters with each parameter representing a rheological factor but details of the Rheality™ Gamma function and the process of classification is currently protected by Patent Cooperation Treaty under publication number WO 2020/260889 A1.

Each experimental process condition as outlined in Table 3-1 was run in triplicate so the data processing for each experimental process condition produced a *10×300* RRF™ data matrix. Since it had been established previously as given in Figure 3-7 that even a buffer size of 10 was sufficient to represent stable acoustic readings, the *10×300* RRF™ data matrix was then put into a random sampling function to randomly pick a set of *10×10* RRF™ data and average it. This random sampling was repeated 100 times to generate a new set of *10×100* RRF™ data matrix to represent that sample fluid at the chosen process condition, e.g. a *10×100* RRF™ data matrix for a sample of Glycerol at 30 °C and 29.5 s^{-1} shear rate. This process was repeated for all fluid samples and process conditions tested as outlined in Table 3-1. Table 3-2 shows an example of what the input data matrix looks like and due to the size of the matrix (for a *10×100* matrix size for each process condition with an average of 8 process conditions per fluid sample tested, the matrix becomes *10×800* for one fluid), it is not possible to present the matrix data result in report form. Also, the data matrix is only useful for training the supervised machine learning model or averaging down the matrix and transforming it into a stacked bar plot as shown in Figure 3-6.

RRF Parameter	Buffer 1	Buffer 2	Buffer 3	Buffer 4	Buffer 5	Buffer 6	Buffer 7	Buffer 8	Buffer ….
P1	1.803	1.789	1.796	1.794	1.799	1.801	1.796	1.799	….
P2	0.625	0.620	0.619	0.619	0.620	0.620	0.618	0.620	….
P3	0.203	0.201	0.200	0.200	0.200	0.201	0.201	0.202	….
P4	0.125	0.124	0.123	0.123	0.123	0.124	0.124	0.125	….
P5	0.097	0.097	0.096	0.096	0.096	0.097	0.097	0.098	….
P6	0.097	0.096	0.096	0.096	0.096	0.096	0.097	0.098	….
P7	0.100	0.100	0.099	0.099	0.099	0.099	0.100	0.101	….
P8	0.096	0.096	0.095	0.095	0.095	0.096	0.096	0.097	….
P9	0.099	0.098	0.098	0.097	0.098	0.098	0.099	0.100	….
P10	0.100	0.100	0.099	0.099	0.099	0.099	0.100	0.101	….

Table 3-2: Example of Input Data Matrix for training a supervised model

In order to build up the output matrix, the principle behind supervised machine learning as mentioned in Section 2.4 is recalled. The output data has to be made up of known rheological values and these rheological values have been obtained on the offline rheometer for each sample fluid at the chosen process conditions. The three sample fluids chosen for this study are of three distinct rheological characteristics:

- Glycerol solution which is a Newtonian fluid and obeys the rheological model represented by equation (2-2)
- Carboxymethyl cellulose solution which is a Non-Newtonian fluid and obeys the rheological model represented by equation (2-3)
- Carbopol® solution which is a Non-Newtonian fluid with yield stress and obeys the rheological model represented by equation (2-6)

Although all three fluids obey three different rheological models, all three fluids can be forced into the third model, the Herschel-Bulkley model by forcing rheological values such as the rate index (n) and yield stress (τ_0).

For Glycerol solutions, with rate index (n) forced to 1 and yield stress (τ_0) forced to 0, Herschel-Bulkley model becomes Newtonian model. For Carboxymethyl cellulose solutions, with yield stress (τ_0) forced to 0, Herschel-Bulkley model becomes Power Law model. Based on this, a standard output matrix can be built for each fluid using all three rheological values and taking into account rheological values for Newtonian and Power Law models that have been forced in order to be represented by the Herschel-Bulkley model and an example of the output is shown in Table 3-3. Table 3-3 shows an example of the output data matrix with the three rheological values of viscosity (η), rate index (n) and yield stress (τ_0) used to train the predictive model.

For every input data in the input matrix, there must be a corresponding output data in the data matrix. So, for an input data matrix of *10×100* RRF™ data matrix, the output data matrix must have a corresponding size of *3×100* in the rheological value matrix.

Rheological Values	Buffer 1	Buffer 2	Buffer 3	Buffer 4	Buffer 5	Buffer 6	Buffer 7	Buffer 8	Buffer ….
Viscosity (η)	0.124	0.124	0.124	0.124	0.124	0.124	0.124	0.124	….
Rate Index (n)	0.771	0.771	0.771	0.771	0.771	0.771	0.771	0.771	….
Yield Stress (τ_0)	3.526	3.526	3.526	3.526	3.526	3.526	3.526	3.526	….

Table 3-3: Example of Output Data Matrix for training a supervised model

In deciding on the makeup of the data matrix for both input and output values for each fluid, the following considerations were made and results discussed later in Section 4.3.2:

For the Glycerol solution which had only two process changes, i.e. temperature and shear rate,

- Build the training matrix with input and output data for the different temperatures tested on a single selected shear rate, i.e. a training matrix with constant shear rate and changing temperature;
- Build the training matrix with input and output data for all the different shear rates and different temperatures tested, i.e. a training matrix with all process conditions tested for Glycerol solution;
- Build a universal training matrix with input and output data for Glycerol, Carboxymethyl cellulose and Carbopol solutions data for all temperatures, concentrations but constant shear rate.

For the Carboxymethyl cellulose solution which had three process changes, i.e. concentration, temperature and shear rate,

- Build the training matrix with input and output data for all concentrations, all temperatures but keep shear rate constant;
- Build the training matrix with both Carboxymethyl cellulose and Carbopol® solutions data for all concentrations, all temperatures but keep shear rate constant;
- Build a universal training matrix with input and output data for Glycerol, Carboxymethyl cellulose and Carbopol solutions data for all temperatures, concentrations but constant shear rate.

For the Carbopol® solution, similar to Carboxymethyl cellulose, the consideration was same,

- Build the training matrix with input and output data for all concentrations, all temperatures but keep shear rate constant;
- Build the training matrix with both Carboxymethyl cellulose and Carbopol® solutions data for all concentrations, all temperatures but keep shear rate constant;
- Build a universal training matrix with input and output data for Glycerol, Carboxymethyl cellulose and Carbopol solutions data for all temperatures, concentrations but constant shear rate.

The Neural Net Fitting app on MATLAB R2020a (MathWorks Inc, USA) was then used to train the predictive model using the RRF™ data matrix as the input and the rheological values (viscosity, rate index and yield stress) data matrix as the output as shown in Figure 3-10 for all the considerations listed above.

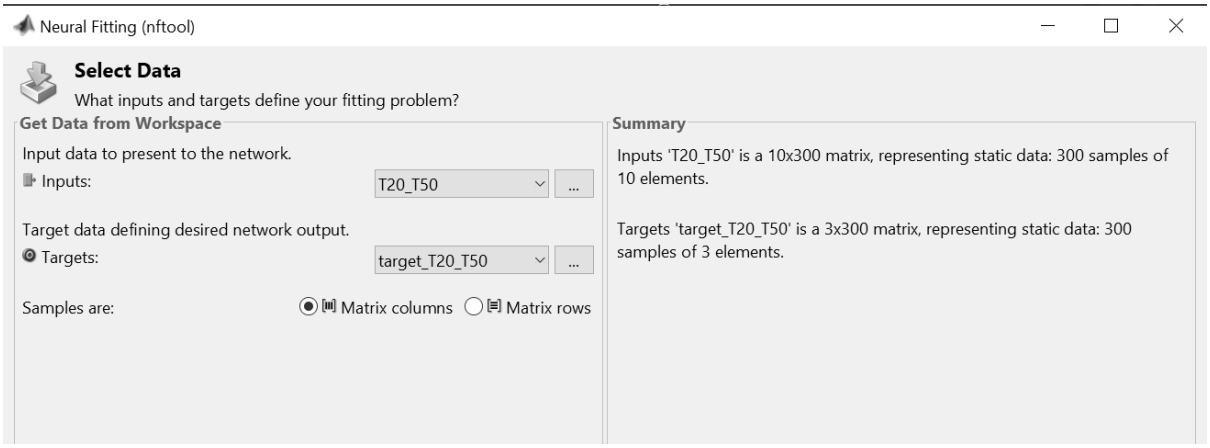

Figure 3-10: Neural Net Fitting on MATLAB R2020a (MathWorks Inc, USA)

The Neural Net Fitting generated a function from the trained model that could then be used to predict rheological values for unknown fluids. As the RRF™ parameters are able to distinguish between Newtonian and Non-Newtonian fluids, sample frequency spectrums for Newtonian fluids are not mixed in the same matrix as Non-Newtonian fluids as they do not obey the same rheological model.

Fluids of "unknown" process conditions were then circulated in the experimental rig (Figure 3-2) and its acoustic signals was then processed into a frequency spectrum and RRF™ parameters. The trained model function was then used to predict the rheological values (viscosity, rate index and yield stress) of the unknown fluid using the RRF™ parameters of the unknown fluid.

4 RESULTS & DISCUSSION

4.1 PRELIMINARY WORK – OFFLINE RHEOLOGY MEASUREMENT

Standard rheological values were first obtained on the offline rheometer (Figure 3-3) by employing experimental methods as outlined in Section 3.3.1. Figure 4-1 shows the analysis of variance for multiple repetition of Glycerol sample at different temperatures. It can be seen that at lower temperatures, the variance in measurements is much greater than at higher temperatures. For rotational rheometers, the experimental error in viscosity measurement is typically within the range of 1 to 10% (Laun, et al., 2014) and the results shown in Table 4-1 show an experimental error range of between 0.2% and 3% when compared to the viscosities calculated in Figure 4-2(a).

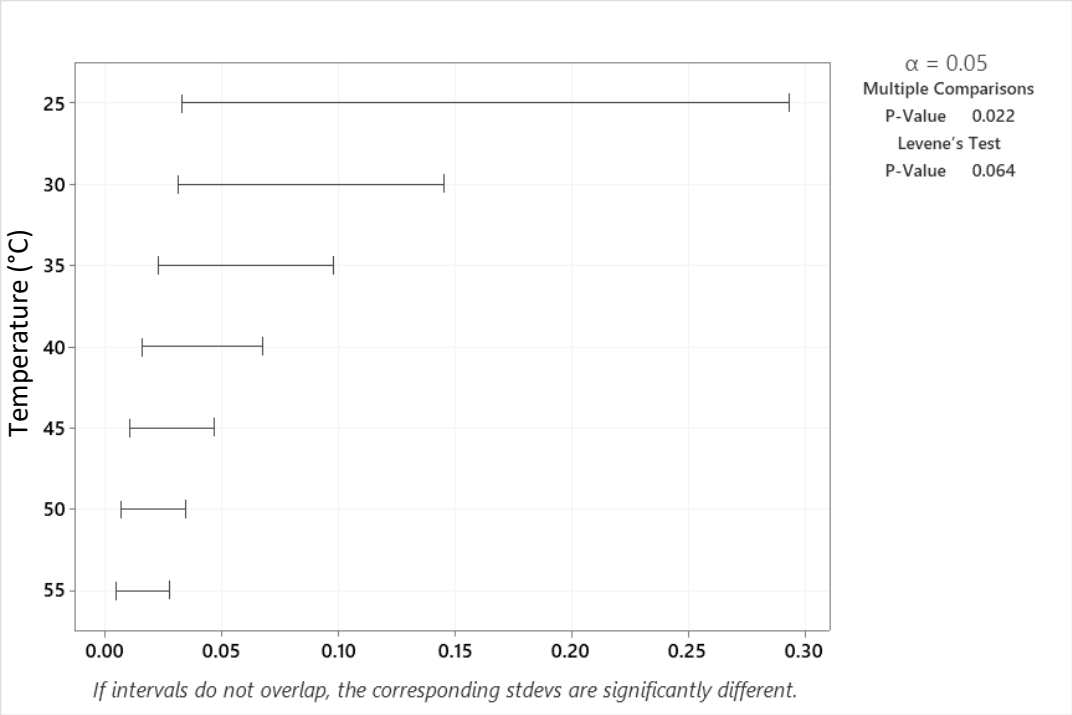

Figure 4-1: Analysis of variance for 5 experimental repetitions to understand reliability of each measurement on the offline rheometer at different temperatures.

4.1.1 GLYCEROL SOLUTION

For Glycerol, three desired temperature of 20, 35 and 50 °C were chosen to serve as reference process conditions and a flow sweep analysis was carried out on sample solutions of Glycerol at each of the chosen temperatures. The shear rates were calculated by applying equation (2-7) to the flow rate values measured by the oval gear flowmeter on the experimental rig (Figure 3-2).

Figure 4.2(a) shows the resulting plot of shear stress versus shear rate for Glycerol solution at three different temperatures of 20 °C, 35 °C and 50 °C and the resultant viscosity at each temperature is 629 mPa.s, 213 mPa.s and 91 mPa.s respectively. The relationship plot of shear stress versus shear rate in Figure 4-1 shows a direct relationship between shear stress and shear rate and confirms Glycerol solution as a Newtonian fluid. The slope of each relationship plot represents the viscosity of the fluid sample at the chosen temperature. As temperature increases, the kinetic energy in the fluid molecules increases and surface tension decreases as the molecules now start to move around more and the intermolecular forces between the molecules

decreases. As surface tension decreases, it is expected that the fluid flows more freely, hence less viscous. Figure 4-2(b) shows the relationship between viscosity and temperature for Glycerol solution and it can be seen that the viscosity decreases as the temperature of the Glycerol solution is increased.

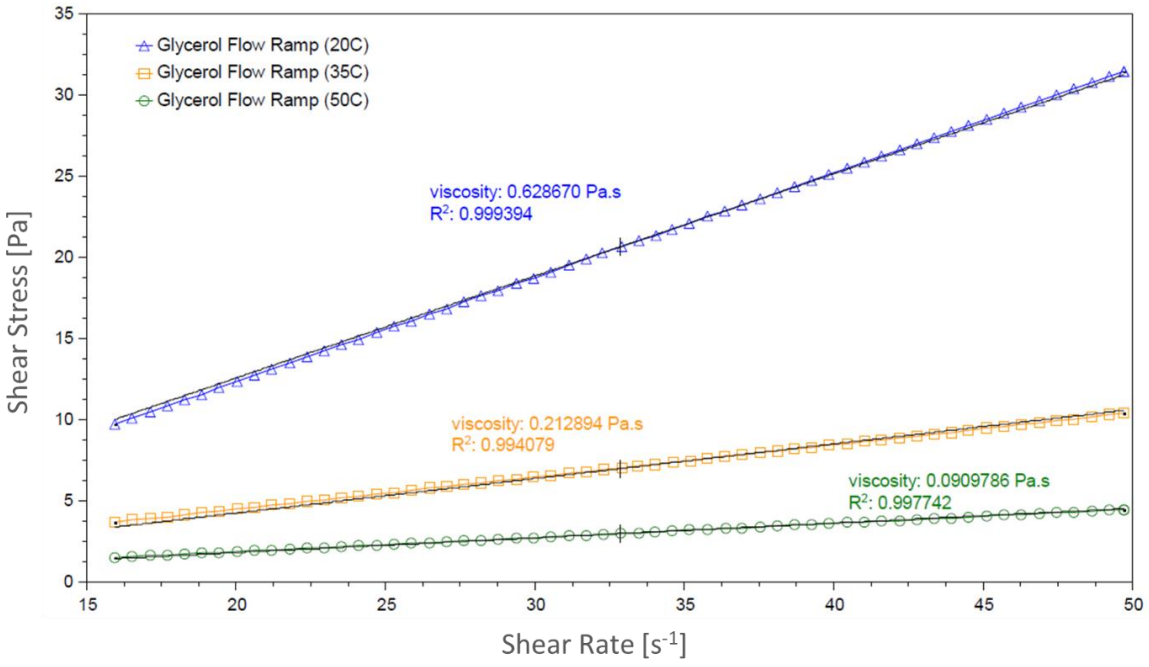

(a)

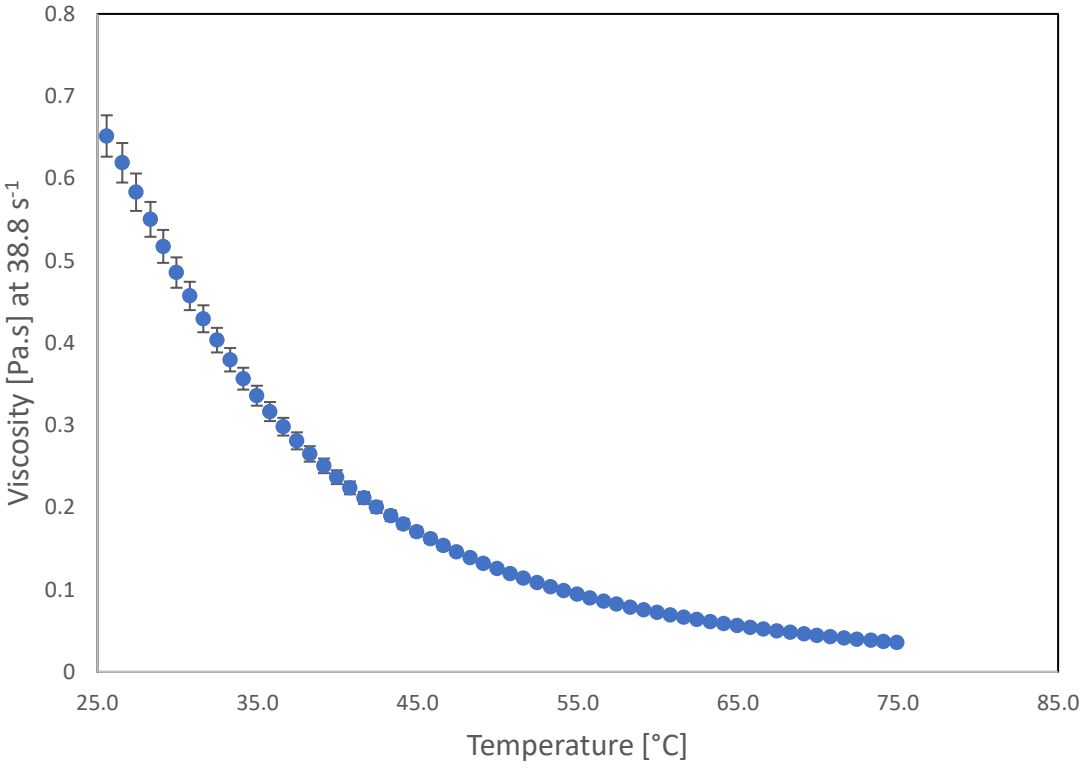

(b)

Figure 4-2: Rheological plots for Glycerol where (a) shows the Shear stress vs shear rate plot for Glycerol solution obtained from the offline rheometer at 3 desired temperatures of 20 °C, 35 °C and 50 °C giving viscosities of 629 mPas, 213 mPas and 91 mPas respectively; and (b) shows the Viscosity vs Temperature curve for Glycerol solution obtained from the offline rheometer at shear rate of 38.8 s^{-1}

Table 4-1 is a summary of rheological values, including viscosity or consistency index, yield stress and rate index, obtained for Glycerol solutions at the desired temperatures and shear rate. As mentioned in Section 3.3.7, in order to maintain a standard three value output, the Herschel-Bulkley equation is forced on Glycerol solution with rate index (n) forced to 1 and yield stress (τ_0) forced to 0 in Equation 2-6. These rheological values will go on to serve as reference values for training and modelling the generated acoustic signal data using Machine Learning.

Material of Choice	Temperature [°C]	Shear rate [s^{-1}]	Viscosity [mPa.s]	Rate Index	Yield Stress [Pa]
Glycerol	20	20.7	616.96	1	0
Glycerol	21	20.7	616.22	1	0
Glycerol	21	29.5	614.51	1	0
Glycerol	30	20.7	334.78	1	0
Glycerol	30	29.5	323.55	1	0
Glycerol	35	20.7	223.60	1	0
Glycerol	35	29.5	216.18	1	0
Glycerol	35	38.8	211.71	1	0
Glycerol	40	20.7	167.51	1	0
Glycerol	40	29.5	161.52	1	0
Glycerol	44	20.7	128.60	1	0
Glycerol	50	20.7	94.54	1	0
Glycerol	50	29.5	91.75	1	0
Glycerol	50	38.8	90.65	1	0
Glycerol	50	49.2	89.95	1	0

Table 4-1: Summary of rheological values for Glycerol solutions at different conditions of temperature and shear rate based on Herschel-Bulkley model where rate index has a value of 1 and yield stress has a value of 0.

4.1.2 CARBOXYMETHYL CELLULOSE SOLUTION

Standard rheological values were also obtained on the offline rheometer for solutions of Carboxymethyl Cellulose (CMC). Desired temperature conditions chosen were between the range of 24 to 51 °C to serve as reference process conditions and a flow sweep analysis was carried out on sample solutions of Carboxymethyl cellulose at each of the chosen temperatures. The result of each flow sweep is a relationship plot showing viscosity, shear stress and shear rate values for the sample fluid. Each relationship plot was then analysed using TRIOS software to determine Power Law coefficients for the resulting curve.

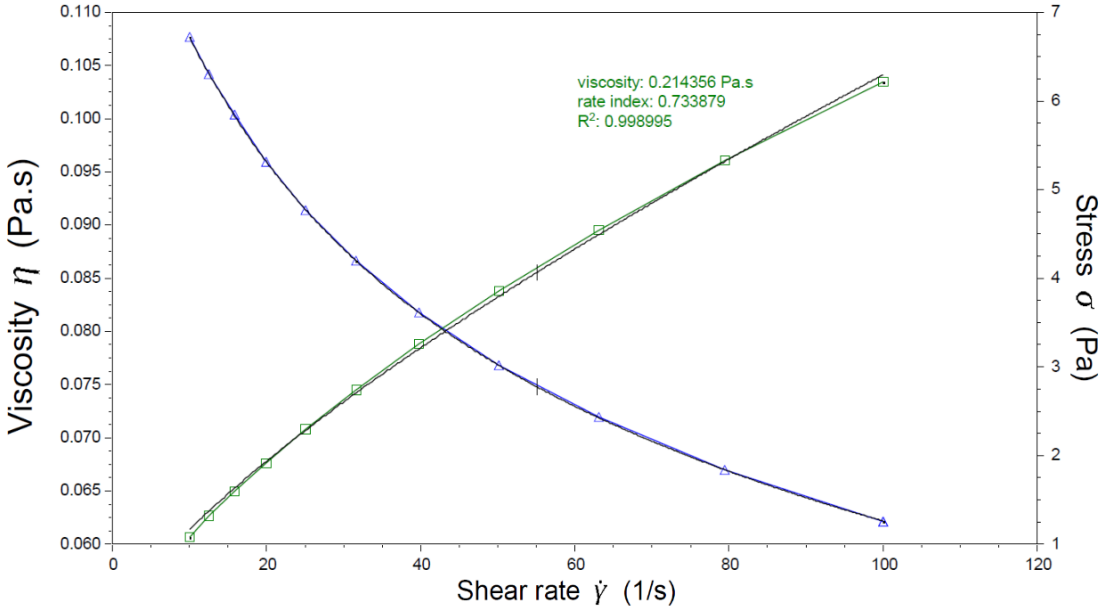

Figure 4-3: Rheological curve of 0.5 wt.% Carboxymethyl cellulose solution showing relationship between shear stress and shear rate and relationship between viscosity and shear rate at 35 °C obtained from the offline Rheometer

Figure 4-3 shows the flow sweep relationship plot for a sample of 0.5 wt.% Carboxymethyl cellulose solution at temperature of 35 °C with one curve representing the relationship between viscosity and shear rate and the second curve representing the relationship between shear stress and shear rate. Each curve has been analysed using the Power Law model to determine its rheological values (viscosity, rate index and yield stress). From Figure 4-3, it can be seen that the shear stress versus shear rate relationship is not a straight-line relationship and viscosity is not constant as shear rate changes but viscosity decreases as shear rate increases which is a character of a shear thinning fluid, confirming that solutions of Carboxymethyl cellulose are Non-Newtonian fluids. Figure 4-4 shows the flow sweep curves of 0.5 wt.% solutions of Carboxymethyl cellulose at different temperatures of 24 °C, 35 °C and 50 °C and it can be seen here that viscosity decreases as temperature of the solution increases.

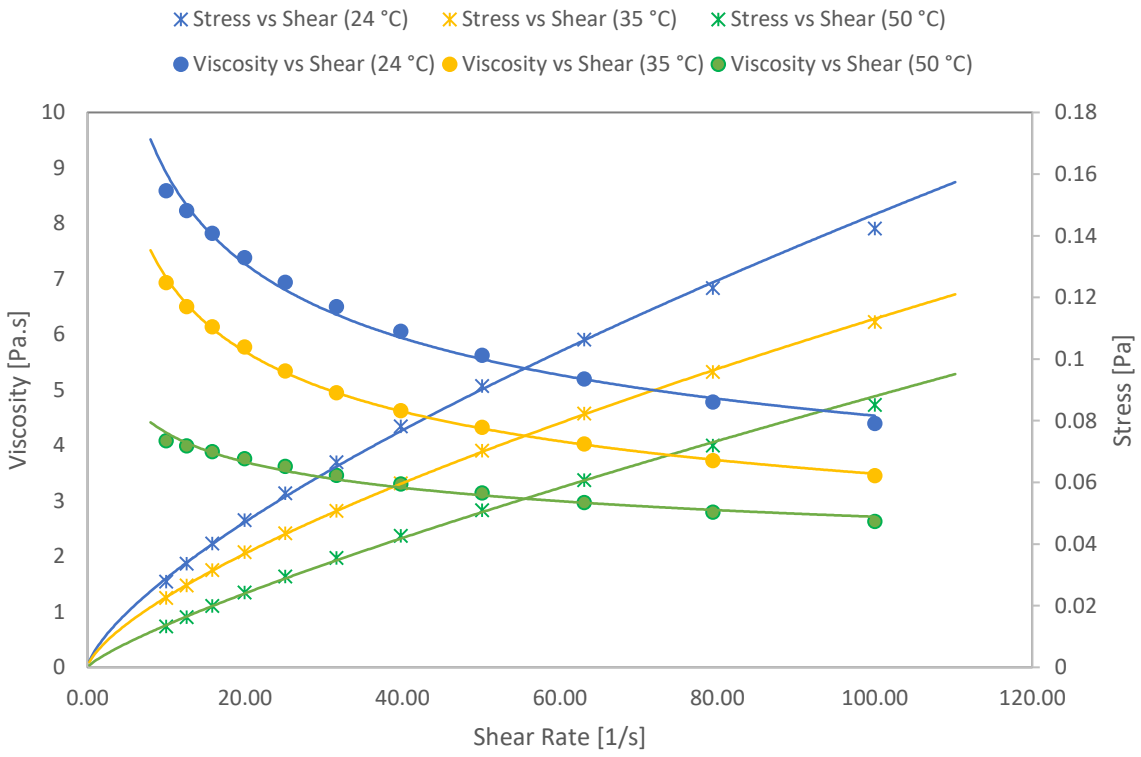

Figure 4-4: Rheological curve of 0.5 wt.% Carboxymethyl cellulose solution showing relationship between shear stress and shear rate and relationship between viscosity and shear rate at temperatures of 24, 35 and 50 °C

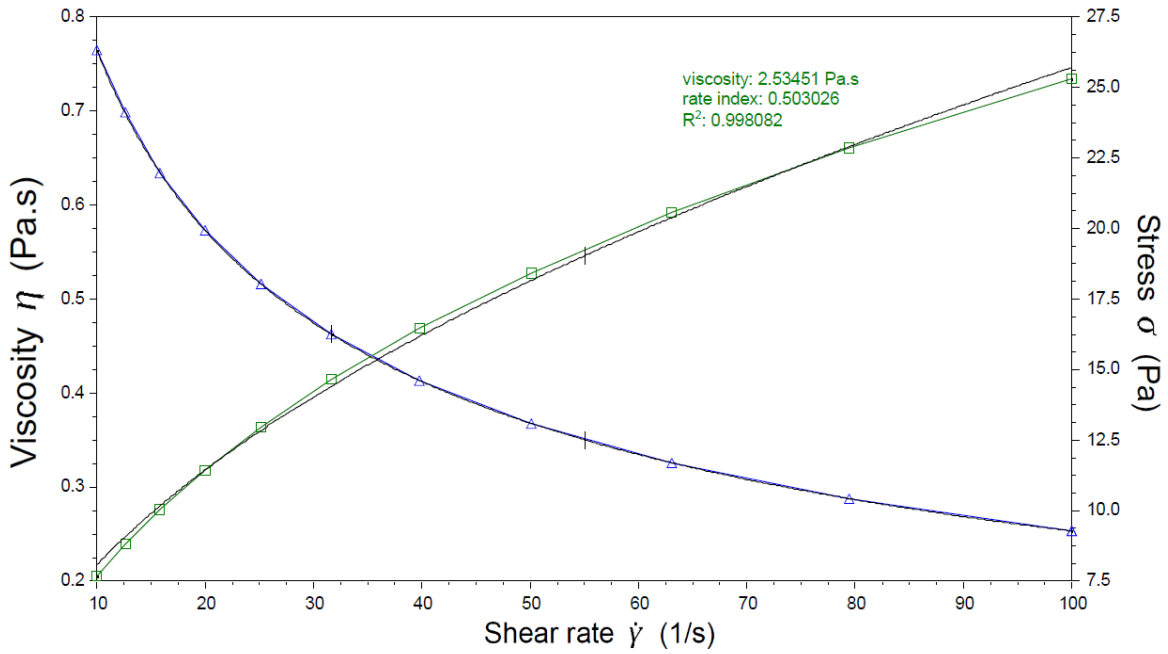

Figure 4-5: Rheological curve of 0.75 wt.% Carboxymethyl cellulose solution showing relationship between shear stress and shear rate and relationship between viscosity and shear rate at desired temperature of 35 °C

Figure 4-5 shows the flow sweep curve of a higher concentration of 0.75 wt.% of Carboxymethyl cellulose at temperature of 35 °C which also obeys the Power Law model as the lower concentration but shear stress and viscosity are higher at similar shear rates as seen

in Table 4-2, so different concentrations of the same fluid in the same fluid phase is expected to obey the same rheological characteristics.

Material of Choice	Temperature [°C]	Shear rate [s^{-1}]	Viscosity [mPa.s]	Rate Index	Yield Stress [Pa]
CMC 0.50 wt.%	24	38.8	108.42	0.68	0
CMC 0.50 wt.%	24	46.6	101.00	0.68	0
CMC 0.50 wt.%	24	53.1	100.00	0.68	0
CMC 0.50 wt.%	35	38.8	81.75	0.69	0
CMC 0.50 wt.%	35	46.6	78.20	0.69	0
CMC 0.50 wt.%	35	53.1	76.00	0.69	0
CMC 0.50 wt.%	50	46.6	60.00	0.78	0
CMC 0.50 wt.%	50	53.1	57.40	0.78	0
CMC 0.75 wt.%	32	38.8	440.00	0.49	0
CMC 0.75 wt.%	32	46.6	400.00	0.49	0
CMC 0.75 wt.%	35	46.6	392.00	0.50	0
CMC 0.75 wt.%	40	46.6	368.00	0.53	0
CMC 0.75 wt.%	46	46.6	360.00	0.55	0
CMC 0.75 wt.%	50	46.6	275.00	0.56	0

Table 4-2: Summary of rheological values for Non-Newtonian Carboxymethyl Cellulose (CMC) solutions at different conditions of concentration, temperature and shear rate

Table 4-2 shows a summary of the rheological values (viscosity, rate index and yield stress) obtained for 0.5 wt.% and 0.75 wt.% solutions of Carboxymethyl cellulose at different process conditions that will serve as the output data for training the supervised machine learning model later discussed in Section 4.3.2. As Figures 4-3, 4-4 and 4-5 have established solutions of Carboxymethyl cellulose as Non-Newtonian fluids obeying Power Law, yield stress can be represented as $\tau_0 = 0$ when modelled using the Herschel-Bulkley equation.

4.1.3 CARBOPOL® SOLUTION

Standard rheological values were also obtained for the solutions of Carbopol. Flow sweep analysis was carried out on sample solutions of Carbopol at desired temperatures between a range of 24 to 51 °C. The result of each flow sweep is a rheological plot showing viscosity, shear stress and shear rate values for the sample fluid. Each relationship plot was then analysed using the Herschel-Bulkley model on the TRIOS software to determine the rheological coefficients for the resulting curve.

Figure 4-6 shows the resulting rheological plot for a 0.25 wt.% solution of Carbopol at 45 °C and it can be seen that the shear stress versus shear rate relationship is not a linear relationship so solutions of Carbopol are not Newtonian fluids. Also worthy of note on Figure 4-6 is the presence of a yield stress. At $\dot{\gamma} = 0$, shear stress is not equal to zero as was observed with solutions of Carboxymethyl cellulose in Figure 4-4 but a minimum shear stress value is observed that must be overcome before the fluid starts to move. This implies that solutions of Carbopol® can be successfully modelled using the Herschel-Bulkley equation.

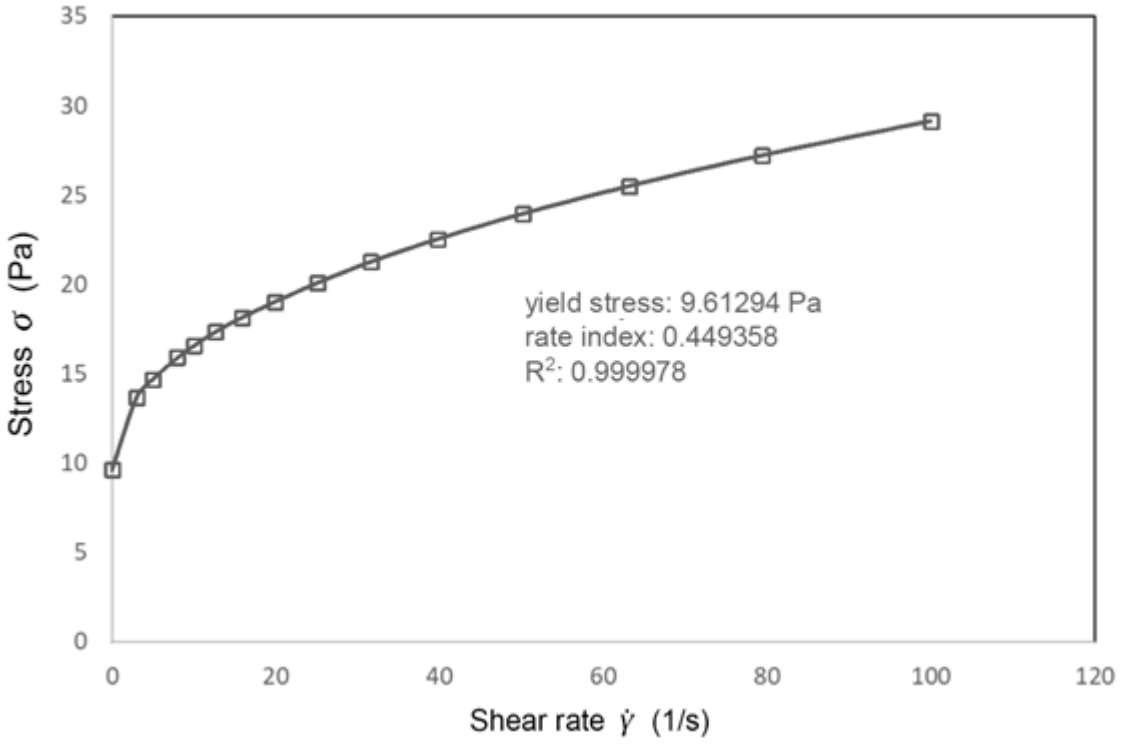

Figure 4-6: Rheological curve of 0.25 wt.% Carbopol solution showing relationship between shear stress and shear rate at temperature of 45 °C

Material of Choice	Temperature [°C]	Shear rate [s^{-1}]	Viscosity [mPa.s]	Rate Index	Yield Stress [Pa]
Carbopol 0.10 wt.%	21	40.6	43.50	0.71	0.057
Carbopol 0.10 wt.%	21	46.6	42.00	0.71	0.057
Carbopol 0.10 wt.%	21	53.1	40.10	0.71	0.057
Carbopol 0.10 wt.%	35	46.6	29.40	0.71	0.044
Carbopol 0.10 wt.%	45	46.6	25.70	0.72	0.037
Carbopol 0.10 wt.%	50	46.6	24.00	0.72	0.028
Carbopol 0.25 wt.%	29	40.6	608.60	0.45	9.25
Carbopol 0.25 wt.%	29	46.6	562.20	0.45	9.25
Carbopol 0.25 wt.%	29	53.1	510.00	0.45	9.25
Carbopol 0.25 wt.%	45	46.6	522.00	0.45	8.61
Carbopol 0.25 wt.%	51	46.6	466.00	0.42	8.10

Table 4-3: Summary of rheological values for Non-Newtonian with yield stress Carbopol solutions at different conditions of concentration, temperature and shear rate

Table 4-3 shows a summary of rheological values (viscosity, rate index and yield stress) for 0.1 wt.% and 0.25 wt.% of Carbopol solutions at different process conditions measured on the offline rheometer which will then serve as the output values for training a supervised machine learning model as later discussed in Section 4.3.2. From Table 4-3, the following can also be deduced:

- For both concentrations of Carbopol, viscosity decreases as temperature increases but the extent of decrease in the lower concentration solution (43% decrease as temperature increased from 21 °C to 50 °C at constant shear rate of 46.6 s^{-1}) is greater than in the higher concentration solution (17% decrease as temperature increased from 29 °C to 51

°C at shear rate of 46.6 s^{-1}). As temperature increases, the hydrogen bonds between both the Carbopol molecules and water molecules become weaker and break (Khan, Hassan, & Pathak, 2015), resulting in a fluid that flows more freely or less viscous but at higher concentration, the increased number of hydrogen bonds means that even at higher temperature, the extent of free flowing, compared to the lower concentration, is reduced;

- Both concentrations of Carbopol solution are shear thinning; as shear rate increases from 40.6 to 53.1 s^{-1} for each temperature, viscosity decreases;
- As concentration increases from 0.1 wt.% to 0.25 wt.%, rate index decreases and the fluid becomes less Newtonian. As temperature increases for each concentration, however, rate index remains fairly constant (Figure 4-7) so temperature has no effect on rate index;
- As temperature increases for both concentrations, yield stress decreases (Figure 4-8) and at lower concentration, the magnitude of reduction in yield stress as temperature increases (± 0.02 Pa) is lower than at higher concentration (± 0.76 Pa). The Arrhenius activation energy theory can be used to explain the relationship between yield stress and temperature (Khan, Hassan, & Pathak, 2015).

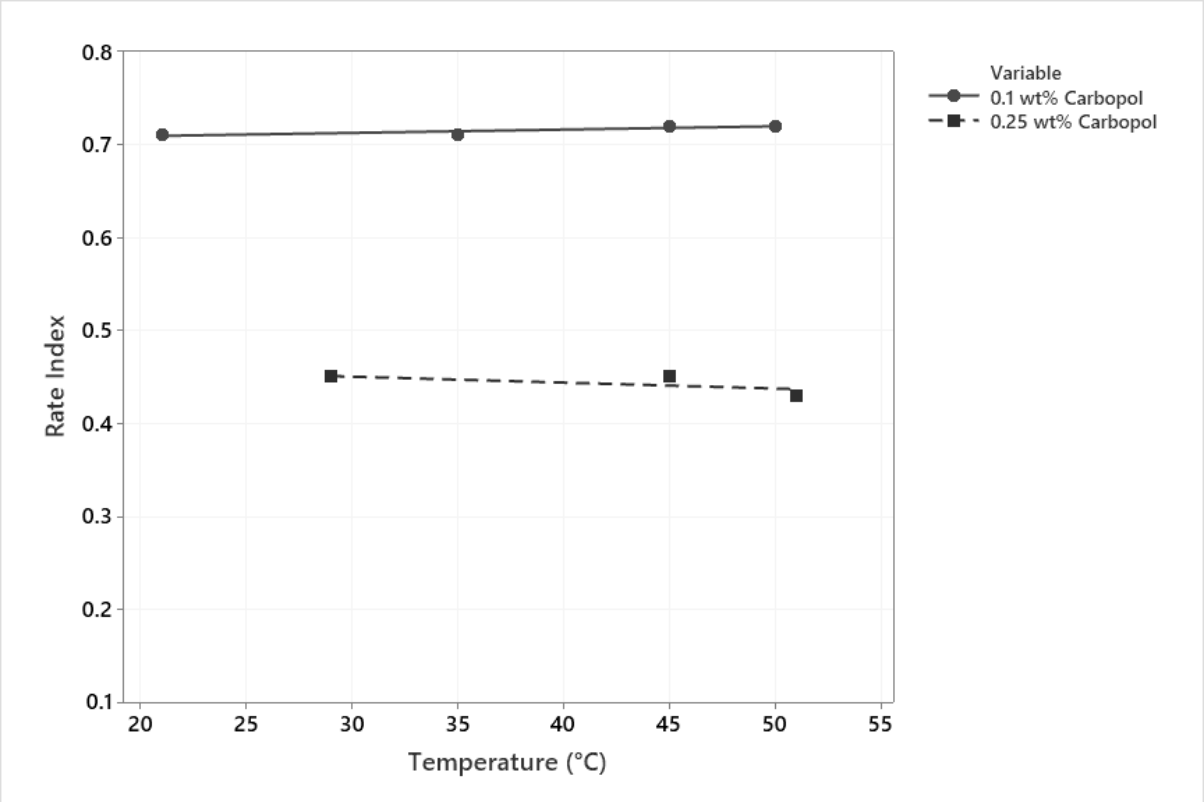

Figure 4-7: Relationship between rate index and temperature for two concentrations of Carbopol solution

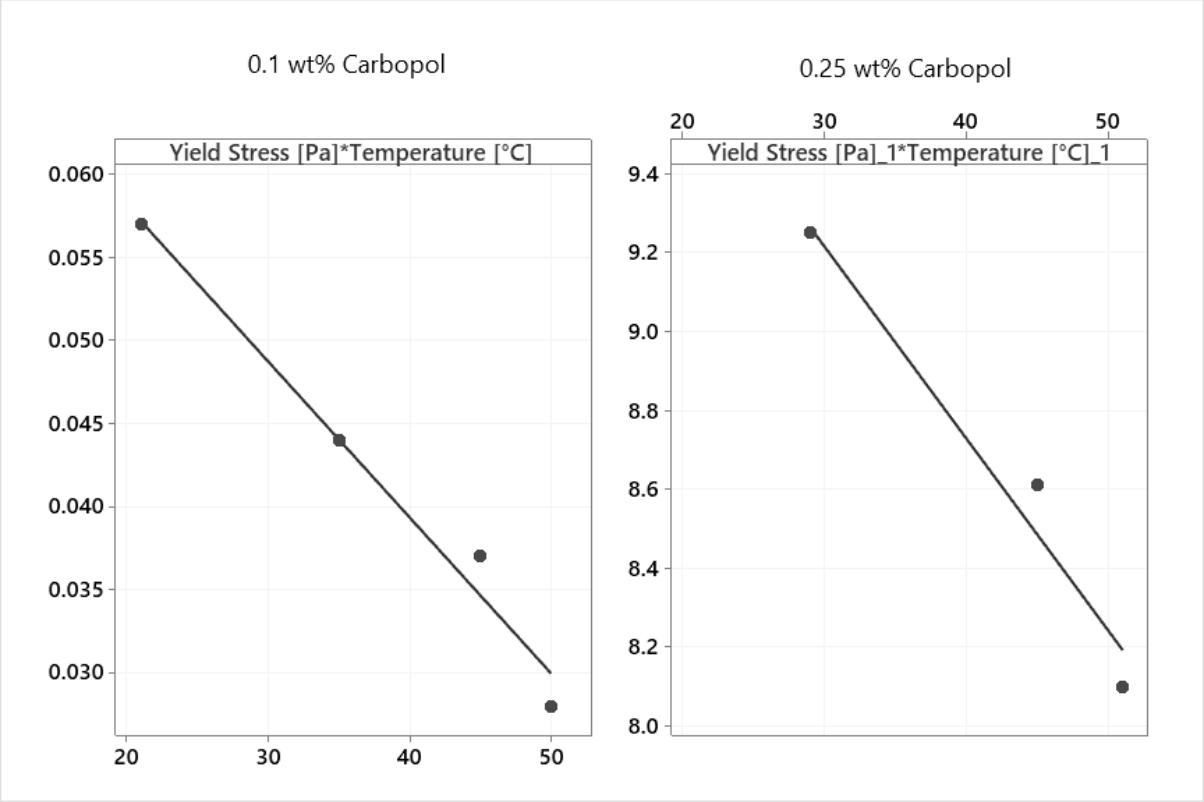

Figure 4-8: Relationship between yield stress and temperature for two concentrations of Carbopol solution

4.2 ONLINE RHEOLOGY MEASUREMENT

One of the limiting factors of Acoustic Emission monitoring is the large amount of data generated which requires an extensive processing time and in order to streamline that data collecting and processing time, preliminary works mentioned in Section 3.3.5 were carried out to establish the leanest possible data size required for stable, reliable signal collection. Another limiting factor was the choice of Glycerol as a fluid to represent Newtonian rheology as Glycerol is hygroscopic in nature. Due to the amount of time spent collecting online rheology data, all experimental process conditions could not be tested and collected on the same day for each fluid and because Glycerol absorbs moisture from the atmosphere, there is a high tendency of compromising the rheology of the Glycerol solution being sampled if the experimental setup is left on standby. Precautions were taken while running Glycerol solutions in the experimental rig to minimise the effects of the hygroscopic nature of Glycerol by ensuring the vessel was air tight but the success of the precautionary measures could only be determined after the data collected for the Glycerol solution runs were completely analysed. Alternative Newtonian fluids to consider include ethanol, glycol, cooking oil, gasoline, silicone oil or motor oil.

Once baseline parameters were established on the experimental setup and reference rheological values had been obtained from the offline rheometer, online acoustic emission signal data was then collected for each sample fluid at conditions listed in Table 3-1 using methods described in Section 3.3.3. The acoustic signals collected were analysed and processed using methods described in Section 3.3.4 to generate Rheological fingerprints for each sample where each rheological fingerprint corresponds to a combination of flow rate/shear and temperature classified into 10 parameters with unique signal intensity. Using these methods, online

rheology measurements were collected for solutions of Glycerol as a Newtonian fluid and solutions of Carboxymethyl Cellulose (CMC) as well as solutions of Carbopol as Non-Newtonian fluids.

4.2.1 NEWTONIAN RHEOLOGY

4.2.1.1 CHANGE IN TEMPERATURE

Figure 4-9 shows an example of the typical analysis result from employing methods described in Section 3.3.4 to determine online rheology measurements obtained by the acoustic sensor for solutions of Glycerol at given process conditions. Figure 4-9 shows the stacked rheological fingerprint made up of the 10 unique rheological parameters that the sampled frequency spectrum had been split into for solutions of Glycerol at a fixed shear rate of 20.7 s^{-1} and varying temperature between 20 °C and 50 °C. It can be seen from Figure 4-9 that each temperature produces a unique set of RRF™ values that distinguishes it from the next set of process conditions. It is also worthy of note that even with temperature changes as little as 5 °C, a unique set of RRF™ values were obtainable. On its own, it is almost impossible to decode rheological values such as viscosity from each set of RRF™ values for a given process condition as it is just a set of frequency spectra that have been classified into the 10 rheological parameters using machine learning but the RRF™ values are able to instantly give visual clues for when a change has occurred in the fluid being measured or monitored. In order to generate rheological values from these frequency spectra, supervised machine learning is used to train a model using the reference rheological values measured from the offline rheometer.

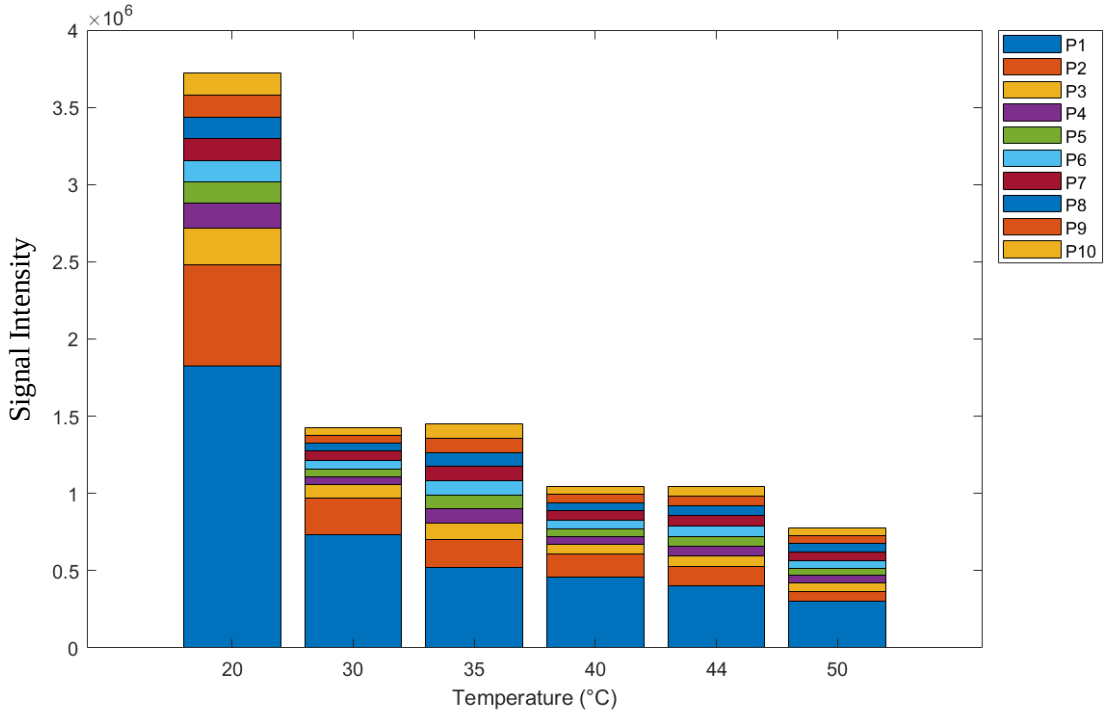

Figure 4-9: Stacked Rheological fingerprint showing sampled frequency spectrum split into 10 unique rheological factors for solutions of Glycerol at a fixed shear rate of 20.7 s^{-1} and different temperatures

4.2.1.2 CHANGE IN SHEAR RATE

Figure 4-10 shows the rheological fingerprint for solutions of Glycerol at a fixed temperature of 50 °C and varying shear rate between 15.5 s^{-1} and 49.2 s^{-1}. It can be seen from Figure 4-10 that each shear rate condition produces a unique set of RRF™ values that distinguishes it from the next set of process conditions as observed with changes in temperature in Figure 4-9. Figure 4-11 shows the rheological fingerprint of all sampled process conditions in a single chart for solutions of Glycerol sampled at different temperatures and shear rate with each stacked bar being the corresponding fingerprint for a particular temperature and shear rate, e.g. 20 [20.7] being rheological fingerprint for Glycerol solution at 20 °C and 20.7 s^{-1}.

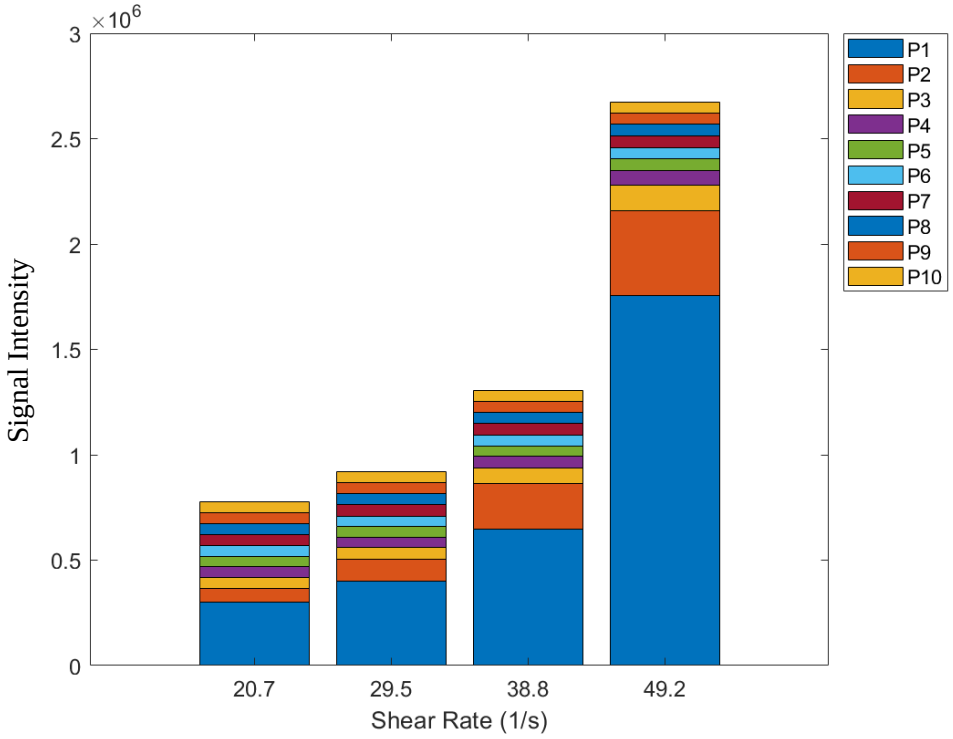

Figure 4-10: Stacked Rheological fingerprint showing sampled frequency spectrum split into 10 unique rheological factors for solutions of Glycerol at a fixed temperature of 50 °C and different shear rates

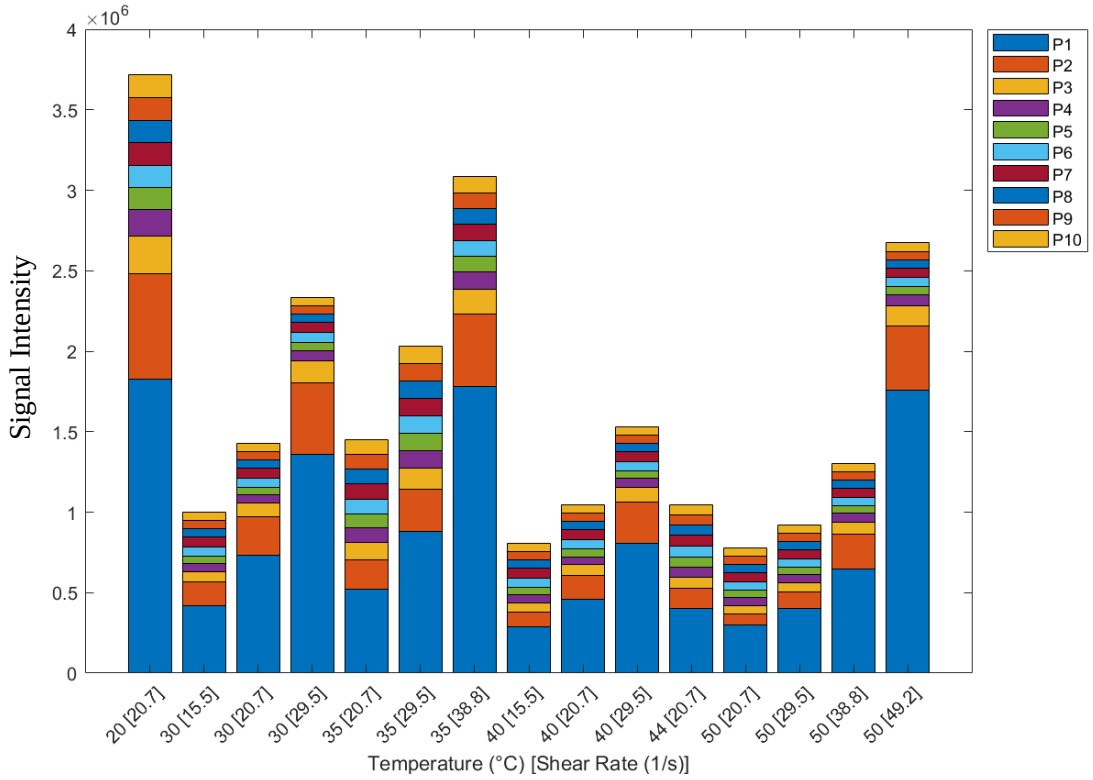

Figure 4-11: Stacked Rheological fingerprint showing sampled frequency spectrum split into 10 unique rheological factors for solutions of Glycerol at all sampled process conditions of different temperatures and different shear rates

4.2.2 NON-NEWTONIAN RHEOLOGY

4.2.2.1 CHANGE IN TEMPERATURE AND SHEAR RATE

Figure 4-12 to 4-15 show the resulting sampled frequency spectra for solutions of Carboxymethyl Cellulose at different process conditions with Figure 4-12 showing distinct rheological factor values for 0.5 wt.% concentration at the same shear rate of 46.6 s^{-1} and different temperatures of 24 °C, 35 °C and 50 °C. Just like it was observed with solutions of Glycerol, a change in fluid temperature results in a change in acoustic signal recorded by the acoustic sensor and after data processing, a visual representation of the change in process condition can be seen.

Figure 4-13 shows a similar result when the concentration of the Carboxymethyl Cellulose solution is changed, in this case from 0.5 wt.% to 0.75 wt.%, however, closer temperature range conditions have been tested with the increased concentration of 0.75 wt.%. It can be seen that rheological factor values for 32 °C and 35 °C here are very close in value and a change here might be lost during the averaging function of the data processing. This result is in tandem with the offline rheology data shown in Table 4-2 which shows only a 2% difference between the viscosity values measured at 32 °C and 35 °C and given that rotational rheometers can have an experimental error range of between 1 to 10% (Laun, et al., 2014), these results could very well fall within error margins of each other. To further elaborate on this averaging function, Figure 4-14 shows the frequency spectra for each of the individual buffers recorded during sampling. As recordings were done in triplicates of 100 buffers per sampling, each process

condition has 300 buffers and comparing the individual buffers for the fluid at 32 °C to the individual buffers for the fluid at 35 °C, it is easy to see how the very small changes can be lost once all 300 buffers are averaged out to present averaged bars as shown in Figure 4-13.

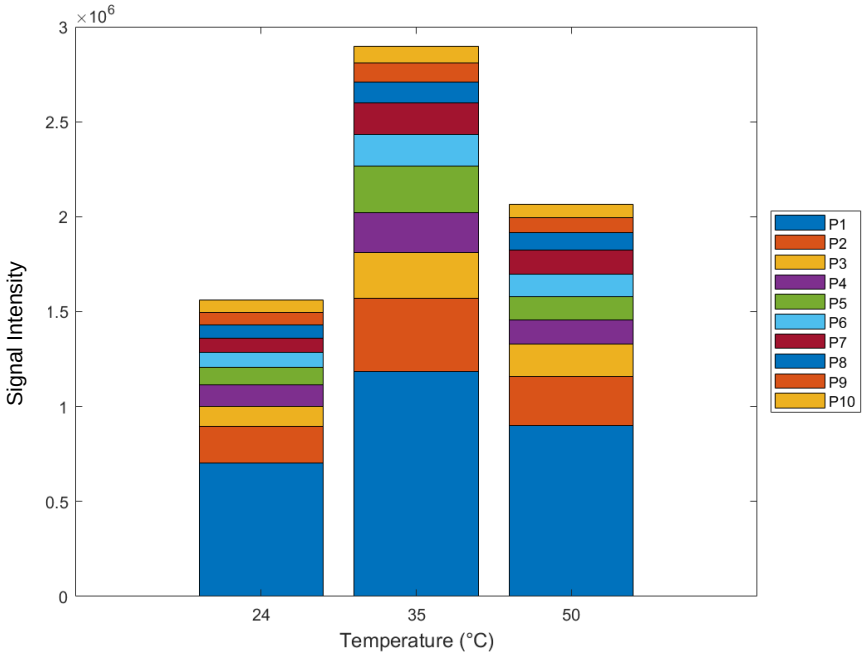

Figure 4-12: Stacked Rheological fingerprint showing averaged sampled frequency spectra for 0.5 wt.% solution of Carboxymethyl Cellulose (CMC) at fixed shear rate of 46.6 s^{-1} and varying temperatures

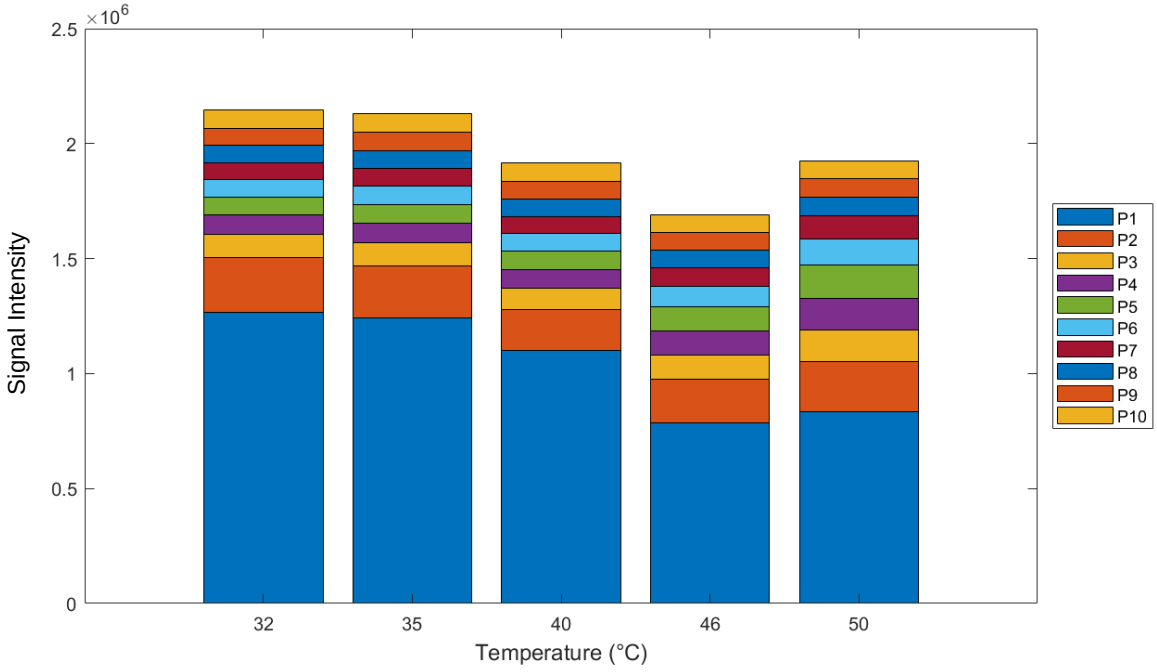

Figure 4-13: Stacked Rheological fingerprint showing averaged sampled frequency spectra for 0.75 wt.% solution of Carboxymethyl Cellulose (CMC) at fixed shear rate of 46.6 s^{-1} and varying temperatures

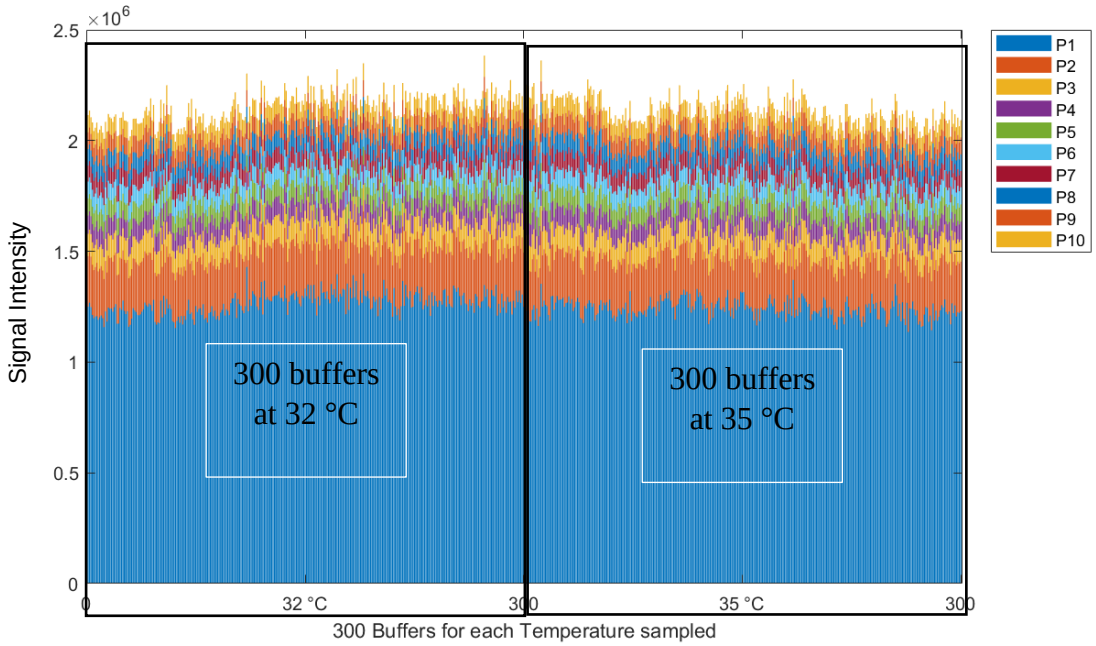

Figure 4-14: Comparison of Rheological fingerprint for instantaneous buffer recorded (before averaging) for 0.75 wt.% solution of Carboxymethyl Cellulose (CMC) at fixed shear rate of 46.6 s^{-1} and temperatures of 32 °C and 35 °C

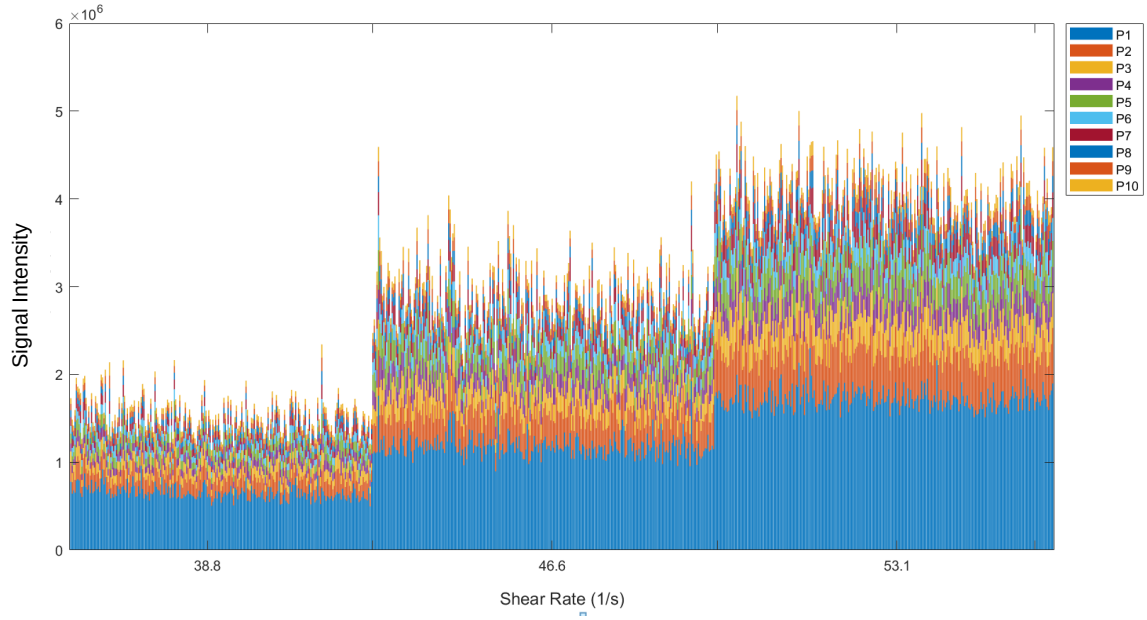

Figure 4-15: Comparison of Rheological fingerprint at different shear rates of 38.8 s^{-1}, 46.6 s^{-1} and 53.1 s^{-1} showing sampled frequency spectra of instantaneous buffer recorded (before averaging) for 0.5 wt.% solution of Carboxymethyl Cellulose (CMC) at fixed temperature of 35 °C

Figure 4-15 shows the instantaneous sampled frequency spectra for individual buffers for 0.5 wt.% solution of Carboxymethyl Cellulose at a fixed temperature of 35 °C while varying shear rate from 38.8 s^{-1} to 53.1 s^{-1} and as it had been seen with solutions of Glycerol, a change in shear rate produces a significantly different set of rheological factor values. It is, however, worthy of note in Figure 4-15 compared to Figure 4-14 that the difference is

significant enough not to be lost during the buffer averaging part of data processing. This level of detailing helps to define levels of sensitivity for the online acoustic monitoring of rheology, i.e. it can be inferred that temperature changes of less than 5 °C cannot easily be differentiated by the device for solutions of Carboxymethyl Cellulose which is same as can be said for an offline rheometer as seen in results presented in Table 4-2.

4.2.2.2 CHANGE IN CONCENTRATION OF FLUID

Figures 4-16 and 4-17 show a like to like comparison of process conditions for different concentrations of the same fluid. At the same temperature and shear rate of 35 °C and 46.6 s^{-1} respectively, 0.5 wt.% concentration of Carboxymethyl Cellulose has a lower viscosity than 0.75 wt.% concentration and both Figures 4-16 and 4-17 show that this difference in viscosity as well as other rheological values can be differentiated by the online acoustic sensor. Figure 4-16 shows the instantaneous frequency spectra for all the individual buffers sampled and a clear distinction can be made for the difference in concentration where the higher concentration solution produces a less noisy frequency spectra. Figure 4-17 shows a comparison of each rheological fingerprint parameter for the averaged frequency spectra at both concentrations to further highlight the distinction that the sensor is able to make of the two fluid samples run at the same process conditions. For each of the 10 rheological parameters, a difference can be spotted between both concentrations.

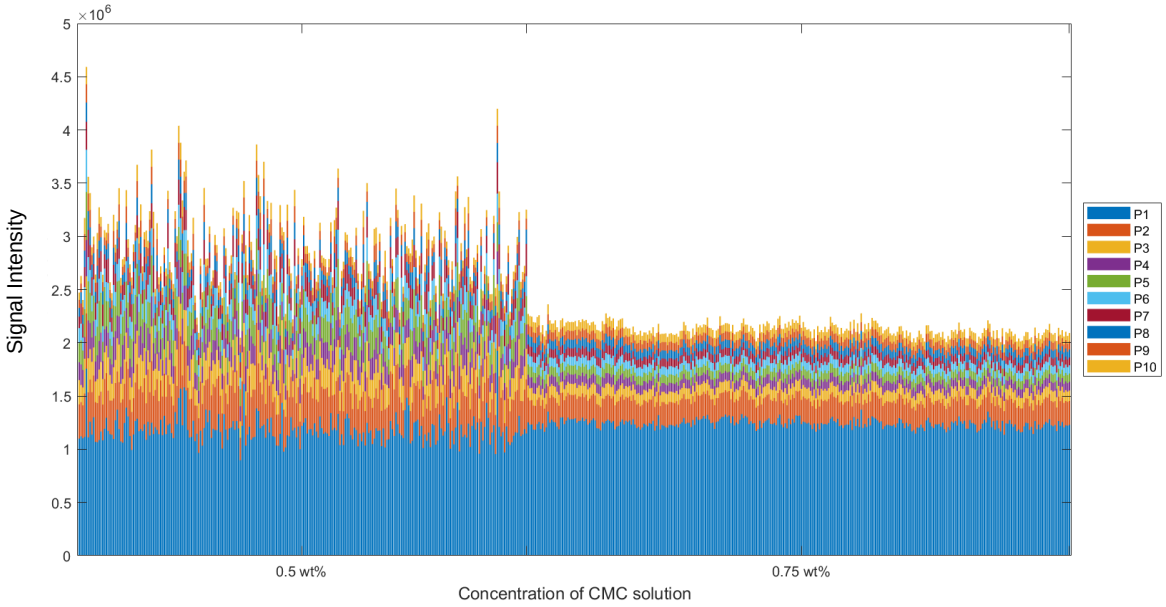

Figure 4-16: Comparison of Rheological fingerprint for instantaneous buffer recording for two different concentrations of Carboxymethyl Cellulose solutions at the same shear rate of 46.6 s^{-1} and same temperature of 35 °C

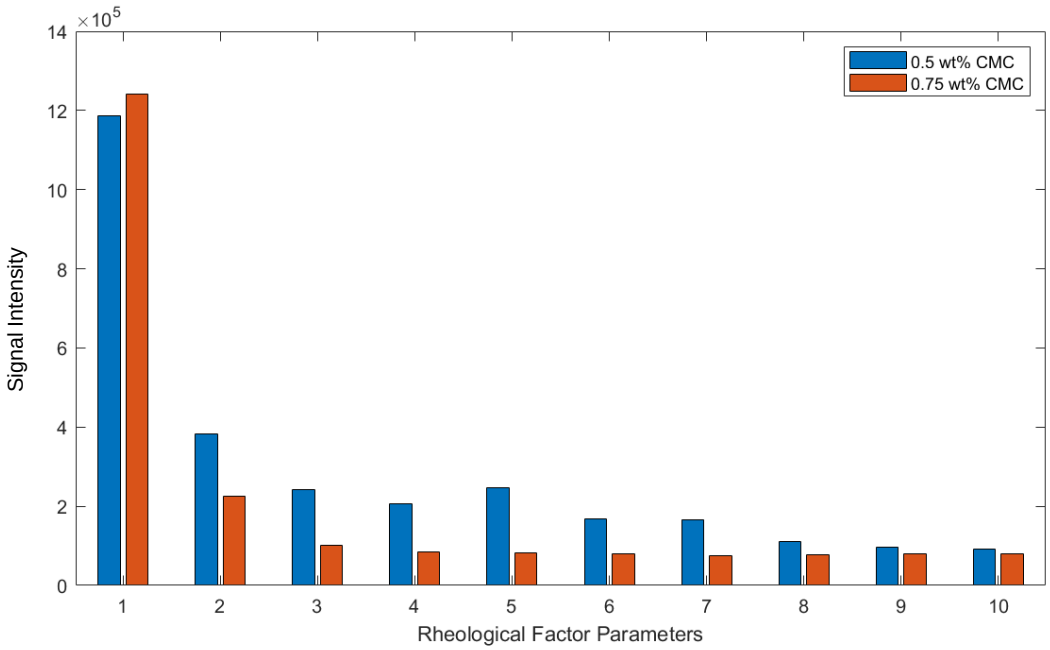

Figure 4-17: Comparison of individual Rheological factor parameters for two different concentrations of the same fluid, solution of Carboxymethyl Cellulose at the same process conditions of 46.6 s^{-1} shear rate and temperature of 35 °C

4.2.3 NON-NEWTONIAN RHEOLOGY WITH YIELD STRESS

The sampled solutions of Carbopol also presented distinct results for changes in temperature, changes in shear rate and changes in concentration of the solution. Figure 4-18 shows the rheological fingerprint parameters for both 0.1 wt.% and 0.25 wt.% concentration of Carbopol on the same plot as temperature was changed while running the samples at identical shear rate of 46.6 s^{-1}. It can be seen in Figure 4-18 that just as it was spotted in Figure 4-13 for Carboxymethyl Cellulose, the sensor is not able to significantly distinguish between Rheological factor values at 35 °C and 45 °C.

Figure 4-19 compares individual rheological fingerprint parameters for a single concentration of Carbopol at the same temperature of 29 °C but at varied shear rates of 40.6 s^{-1}, 46.6 s^{-1} and 53.1 s^{-1}. The results shown in Figure 4-19 are similar to results that had previously been seen with Glycerol and Carboxymethyl Cellulose solutions, showing that the online acoustic sensor is able to produce unique acoustic signals for changing process conditions that can then be processed to generate a rheological factor frequency spectra. These rheological factor frequency spectra can then be used as visual reference limits to monitor a process online or can be further used to train predictive models that would be able to infer actual rheological values for fluid using supervised machine learning.

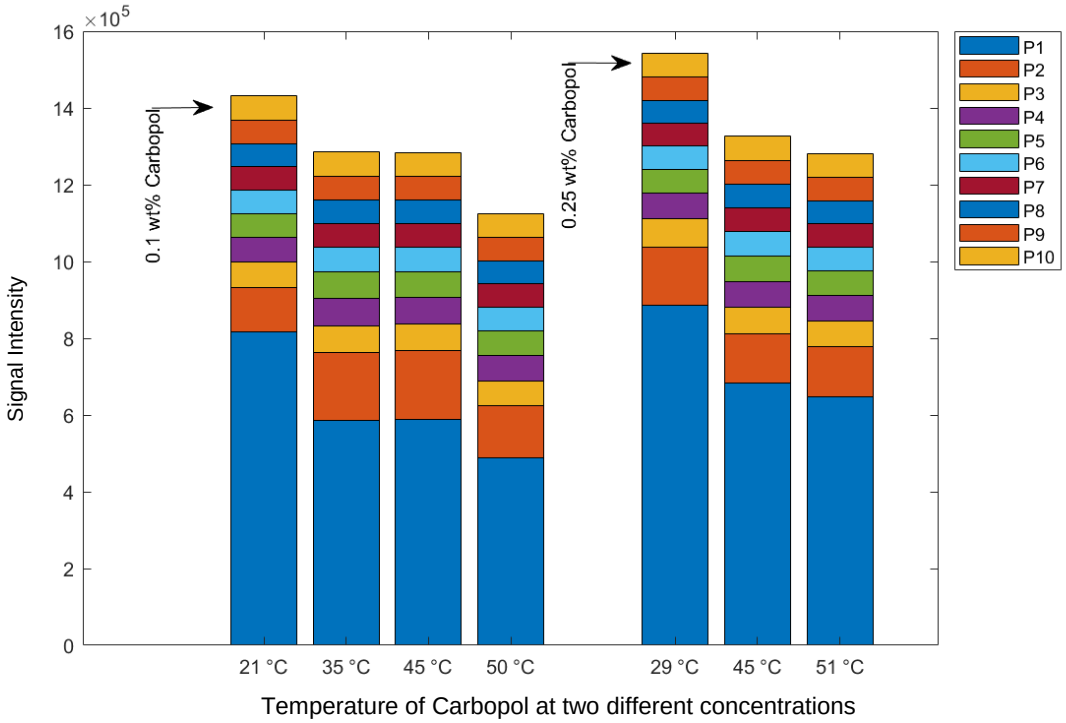

Figure 4-18: Stacked Rheological fingerprints showing sampled frequency spectra for two different concentrations of Carbopol solution at the same shear rate of 46.6 s^{-1} but at different temperatures

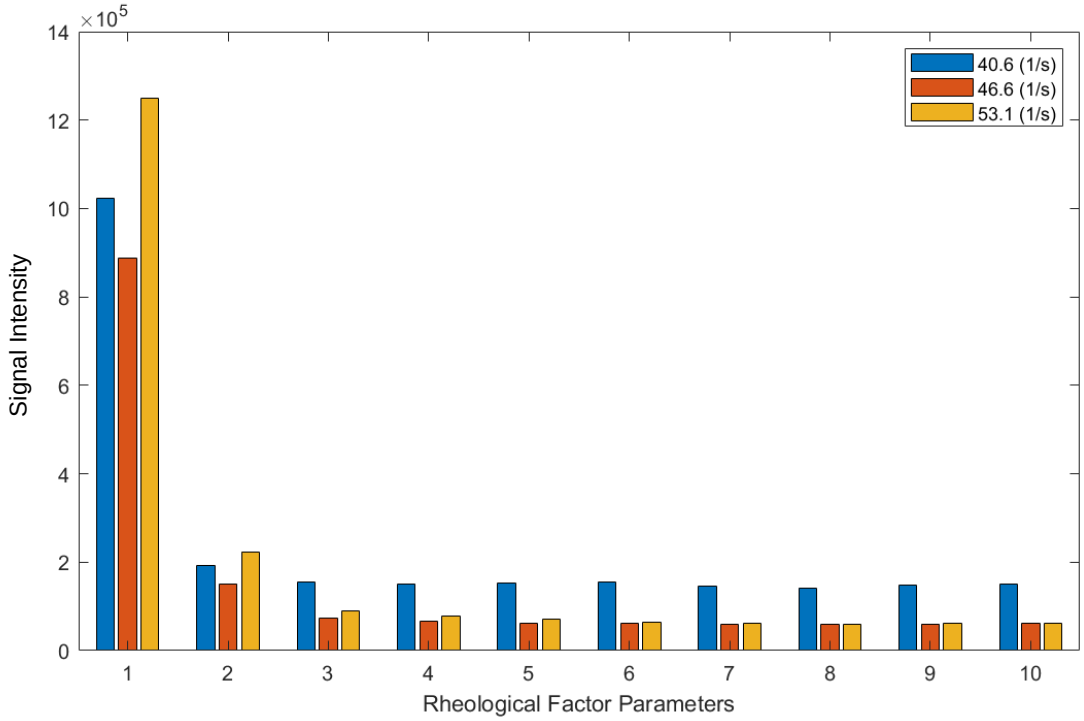

Figure 4-19: Comparison of Rheological factor parameters for solutions of Carbopol at the same concentration of 0.25 wt.% and at the same temperature of 29 °C but at different shear rates

4.3 MACHINE LEARNING TRAINING AND VALIDATION

Section 4.2 covers results from the first set of data processing of acoustic signals recorded by the sensor to determine if the sensor is able to detect a change in signal waves generated that are commensurate with a change in the fluid's rheology and these results have shown that a change can be detected and measured by the online rheology monitoring system. For some instances, detecting and measuring rheological changes might suffice as the process monitoring technique needed, for which, data processing covered by Section 4.2 will suffice but the online rheology monitoring system can go a step further to provide actual rheological values using the principle of inference. This principle of inference is made possible with Supervised Machine Learning as introduced in Section 2.4 where a set of input and its corresponding output is already known and fed into an algorithm to generate a model that would then be able to take new input data and provide output data based on the model developed. In the case of the online rheology system, to transition from a monitoring system to a measuring system, a model is trained using online rheology processed data (the sampled frequency spectrum data) for specific process conditions as the input data and corresponding offline rheometer data as the output data. This known input and output data set is then used to create a matrix which is fed into the algorithm to train a model. Examples of these input and output data matrices are shown in Table 3-2 and Table 3-3.

4.3.1 SUPERVISED MACHINE LEARNING – ARTIFICIAL NEURAL NETWORK

The concept of supervised machine learning using Artificial Neural Network is explained in Section 2.5 where each neuron consists of an input value and a corresponding output value and the neural network is made up of an input, hidden layer and an output layer. In the case of this project work, the online rheology data has an input of 10 which is the 10 unique rheological factor parameters generated from processing each set of acoustic signal data and an output of 3 which is the 3 rheological values being desired in measurement (viscosity, rate index and yield stress) as shown in Figure 3-9.

An example of the input and output data matrix used to train and validate the model is given in Tables 3-2 and 3-3. The result of the training is a MATLAB function that is then expected to generate an output of 3 values whenever an input of 10 Rheological Factor parameters obtained for a given fluid sample is fed into it.

4.3.2 ANN GENERATED FUNCTIONS

A data set matrix was created for each sample of solutions of Glycerol, Carboxymethyl Cellulose and Carbopol at a fixed shear rate and different temperatures. The 10 parameters obtained from each buffer frequency spectra were set as the input data matrix while the 3 rheological values obtained from the offline rheometer were set as the output in the matrix and fed into the Neural Network training tool. An example of the performance of the training model is shown in Figure 4-20. Trained model functions were developed with data sets in this order based on considerations outlined in Section 3.3.7:

- Data Set A – Input and Output data set for Glycerol solutions only
- Data Set B – Input and Output data set for Carboxymethyl Cellulose solutions only
- Data Set C – Input and Output data set for Carbopol solutions only

- Data Set D – Input and Output data set for both Non-Newtonian fluids

(a)

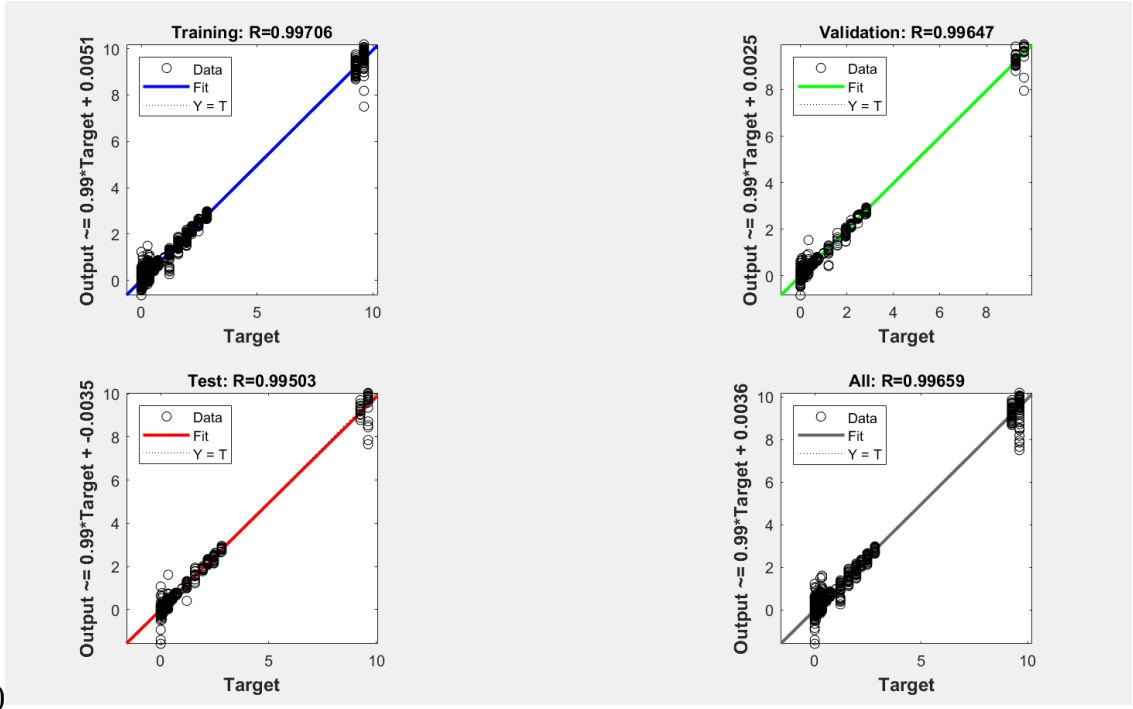

(b)

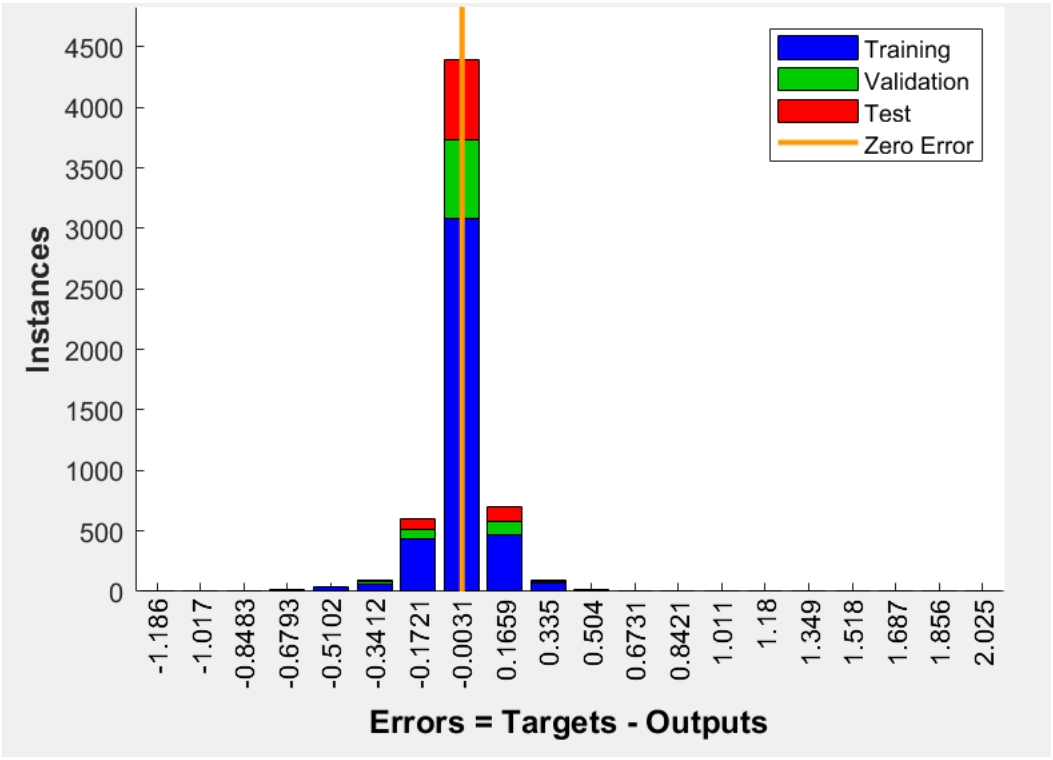

Figure 4-20: Example of model training results (a) regression plots for training, testing and validation data sets showing the performance of the model fit and (b) showing the mean squared error performance of the model trained for Carboxymethyl Cellulose only data set.

Due to the limitations noted in Section 4.2 on the hygroscopic nature of Glycerol, a limited amount of useful data was collected for Glycerol solution and this was not sufficient enough to train a model function for Newtonian rheology so model functions were only developed for Non-Newtonian rheology using data sets for Carboxymethyl cellulose and Carbopol solutions.

The functions developed were then used to determine the rheological values of "unknown" solutions of the sampled fluids and results obtained from the model function was compared with the reference value already obtained from the offline rheometer as shown in Tables 4-4 to 4-7.

	Reference Value	Data Set B Model	Data Set D Model	% Error Data Set B	% Error Data Set D
Yield Stress	0	0	-0.0006		
Viscosity	0.0782	0.0958	0.2907	-23%	-272%
Rate Index	0.6899	0.7713	0.5453	-12%	21%

Table 4-4: Comparison of reference rheological values for sample 0.5 wt.% solution of Carboxymethyl Cellulose at 35 °C obtained from the offline rheometer with rheological values determined by the model functions trained with Data Set B and Data Set D

	Reference Value	Data Set B Model	Data Set D Model	% Error Data Set B	% Error Data Set D
Yield Stress	0	0	4.1184		
Viscosity	0.3680	0.3454	0.6362	6%	-73%
Rate Index	0.5274	0.5507	0.4035	-4%	23%

Table 4-5: Comparison of reference rheological values for sample 0.75 wt.% solution of Carboxymethyl Cellulose at 40 °C obtained from the offline rheometer with rheological values determined by the model functions trained with Data Set B and Data Set D

	Reference Value	Data Set C Model	Data Set D Model	% Error Data Set C	% Error Data Set D
Yield Stress	0.0571	0.0082	0.1760	86%	-208%
Viscosity	0.0257	0.0364	0.0460	-42%	-79%
Rate Index	0.7241	0.7104	0.7382	2%	-2%

Table 4-6: Comparison of reference rheological values for sample 0.1 wt.% solution of Carbopol at 45 °C obtained from the offline rheometer with rheological values determined by the model functions trained with Data Set C and Data Set D

	Reference Value	Data Set C Model	Data Set D Model	% Error Data Set C	% Error Data Set D
Yield Stress	9.2538	9.4779	2.9046	-2%	69%
Viscosity	0.5100	0.5279	0.4547	-4%	11%
Rate Index	0.4528	0.4550	0.4513	0%	0%

Table 4-7: Comparison of reference rheological values for sample 0.25 wt.% solution of Carbopol at 29 °C obtained from the offline rheometer with rheological values determined by the model functions trained with Data Set C and Data Set D

Tables 4-4 and 4-5 show the predictive rheological value results for solutions of Carboxymethyl cellulose at two different concentrations obtained from training two types of model functions developed using Data Set B and Data Set D. It can be seen from both tables that the values closest in range and with the lesser error % to the reference offline rheometer data are those results generated by the Data Set B model function which uses only Carboxymethyl Cellulose data set. This is because all yield stress data in the output matrix of Data Set B can be forced to 0 before training while Data Set D contains sampled Carbopol data which have a yield stress so the trained model is unable to force yield stress to 0 as it is unable to distinguish between Carboxymethyl Cellulose data and Carbopol data in the matrix and would then impose the full Herschel-Bulkley model on Carboxymethyl cellulose and Carbopol data alike.

Tables 4-6 and 4-7 show that using the Data Set D model function (which uses both Carboxymethyl Cellulose and Carbopol data sets) for Carbopol sample fluids produces results that are closer in range compared to Tables 4-4 and 4-5. This is because although Carboxymethyl cellulose data is present in the data set matrix, the presence of non-zero values for yield stress in the matrix means that the machine learning algorithm would take yield stress into account when training to fit the model and the trained model would be a replica of the actual Herschel-Bulkley model but with greater error margins because of the presence of the Carboxymethyl cellulose data. The % error for the lower concentration of both CMC and Carbopol is also seen to be higher because its rheological values are smaller in magnitude compared to the higher concentration.

5 CONCLUSIONS & FUTURE WORK

5.1 CONCLUSIONS

From results discussed in Section 0 of this report, this research work has proven that acoustic signals can indeed be used to detect fluid flow in a pipe and a change in fluid process parameters can be distinguished by such sensors. This research work has also shown limitations in different fluid samples and how sensitivity limits can present through the passive acoustic emission sensor. The acoustic signals generated by the sensor is strong and distinct enough to be used with Mathematical models such as Fast Fourier Transform and Rheality™ Gamma functions to develop a visual monitoring system that can create and detect rheological fingerprints of fluid in process and hence flag non-conforming batches in production.

Results have also shown that besides the development of a monitoring system, Machine Learning tools can be applied to the RRF™ frequency spectra data generated by the system to train and develop a functional model that can predict rheological values for unknown fluids as long as the proper rheological model type is trained. For all the results shown in Tables 4-4 to 4-7, it is clear that in order to properly model and hence predict rheological values, it is better to train models according to the rheological characters of the sampled fluid. Although the output data matrix was established using all three rheological values, forcing the Herschel-Bulkley model to behave as Newtonian (by forcing rate index to 1 and yield stress to 0) and Power Law (by forcing yield stress to 0) model was imperative to the success of those trained models. An alternative approach would be to establish a single value (viscosity) output data matrix for Newtonian fluids, a two-value (viscosity and rate index) output data matrix for Power Law fluids and a three-value (viscosity, rate index and yield stress) output data matrix for Herschel-Bulkley fluids.

5.2 FUTURE WORK

- Now that it has been proven that the Passive Acoustic Emission (PAE) technology can measure signals in both Newtonian and Non-Newtonian fluids, the next step should be to utilise the PAE technology on actual manufacturing process lines and with actual product samples to understand how the technology will cope with real life scenarios as opposed to a controlled environment.
- Although this research work was able to establish the fact that rheological measurements by inference can indeed be made using the PAE technology with machine learning, the results generated by the Artificial Neural Network could be optimised to generate lower error margins and finer prediction values. To do this, one could explore more supervised machine learning algorithms that will produce better results.
- As noted in Figure 2-5 under Section 2.6, the presence of an obstruction within the pipe can amplify the signal generated by the fluid in process. As a follow up work, one could investigate, using computational fluid dynamics, the effects that different shaped obstructions will have on the quality of acoustic signals generated by the fluid and compare how these effects benefit the technology as a whole.

6 REFERENCES

Ahuja, A., & Potanin, A. (2018). Rheological and sensory properties of toothpastes. *Rheologica Acta, 57*(6).

Alberini, F., Hefft, D. I., & Forte, G. (2020). *Great Britain Patent No. WO2020260889A1*.

Aminu, K. T., McGlinchey, D., & Cowell, A. (2019). Acoustic signal processing with robust machine learning algorithm for improved monitoring of particulate solid materials in a gas flowline. *Flow Measurement and Instrumentation, 65*, 33-44.

Ayodele, T. O. (2010). Types of Machine Learning Algorithms. In Y. Zhang (Ed.), *New Advances in Machine Learning* (pp. 19-48). London: IntechOpen. doi:10.5772/9385. 1

Barnes, H. A. (2000). *Handbook of Elementary Rheology.* University of Wales: Institute of Non-Newtonian Fluid Mechanics.

Boyd, J., & Varley, J. (2001). The uses of passive measurement of acoustic emissions from chemical engineering processes. *Chemical Engineering Science, 56*, 1749-1767.

Cady, F. (2017). *The Data Science Handbook.* New Jersey: Wiley.

Chryss, A. G., Monch, A., & Constanti-Carey, K. (2019). Online rheology monitoring of a thickener underflow. *Australian Centre for Geomechanics*.

Darby, R. (2001). *Chemical Engineering Fluid Mechanics* (2 ed.). Taylor & Francis.

George, H. F., & Qureshi, F. (2013). Newton's Law of Viscosity, Newtonian and Non-Newtonian Fluids. In Q. Wang, & Y. Chung (Eds.), *Encyclopedia of Tribology.* Boston, MA: Springer.

Gurney, K. (1997). *An Introduction to Neural Networks.* London: UCL Press.

Habib, M. K., & Chimsom, C. (2019). Industry 4.0: Sustainability and Design Principles. Wels, Austria: IEEE.

Hefft, D. I., & Alberini, F. (2020). A step towards the live identification of pipe obstructions with the use of passive acoustic emission and supervised machine learning. *Biosystems Engineering, 191*, 48-59.

Hefft, D. I., Antonelli, M., & Alberini, F. (2019). Linking Acoustic Emission signals to 2D-PIV results to monitor fluid flow in pipe. Naples: 15th International Conference on Fluid Control, Measurements and Visualization.

Hou, R., Hunt, A., & Williams, R. A. (1999). Acoustic monitoring of pipeline flows: particulate slurries. *Powder Technology, 106*, 30-36.

Javaid, B. (2020). A Strategic Roadmap for the Manufacturing Industry to Implement Industry 4.0. *Designs, 4*(2), 11.

Jimenez, L. N., Martínez Narváez, C. D., Xu, C., Bacchia, S., & Sharma, V. (2021). The rheologically-complex fluid beauty of nail lacquer formulations. *Soft Matter, 17*(20), 5197-5213.

Khan, K., Hassan, M. A., & Pathak, M. (2015). Thermorheological Characterization of Elastoviscoplastic Carbopol Ultrez 20 Gel. *Journal of Engineering Materials and Technology, 137*, 031002-1.

Khulief, Y. A., Khalifa, A., Ben Mansour, R., & Habib, M. A. (2012). Acoustic Detection of Leaks in Water Pipelines using Measurements inside Pipe. *Journal of Pipeline Systems Engineering and Practise, 3*(2), 47-54.

Kwak, M.-S., Ahn, H.-J., & Song, K. (2015). Rheological investigation of body cream and body lotion in actual application conditions. *Korea-Australia Rheology Journal, 27*, 241-251.

Laun, M., Auhl, D., Brummer, R., Dijkstra, D. J., Gabriel, C., Mangnus, M. A., . . . Handge, U. A. (2014). Guidelines for checking performance and verifying accuracy of rotational rheometers: viscosity measurements in steady and oscillatory shear (IUPAC Technical Report). *Pure and Applied Chemistry, 86*(12), 1945-1968.

Li, H., Wang, Y., Zhao, P., Zhang, X., & Zhou, P. (2015). Cutting tool operational reliability prediction based on acoustic emission and logistic regression model. *Journal of Intelligent Manufacturing, 26*, 923-931.

Liu, N., Zhang, D., Gao, H., Hu, Y., & Duan, L. (2021). Real-Time Measurement of Drilling Fluid Rheological Properties: A Review. *Sensors, 21*(11).

Machin, T. D., Wei, H.-Y., Greenwood, R. W., & Simmons, M. J. (2018). In-pipe rheology and mixing characterisation using electrical resistance sensing. *Chemical Engineering Science, 187*, 327-341.

Macosko, C. W. (1996). *Rheology: Principles, Measurements and Applications.* New York: Wiley-VCH.

Malkin, A. Y., & Isayev, A. I. (2012). *Rheology: Concepts, Methods and Applications* (2nd ed.). Toronto: ChemTec Publishing.

Merheb, B., Nassar, G., Nongaillard, B., Delaplace, G., & Leuliet, J. (2007). Design and performance of a low-frequency non-intrusive acoustic technique for monitoring fouling in plate heat exchangers. *Journal of Food Engineering, 82*, 518-527.

Misra, N. N., Sullivan, C., & Cullen, P. J. (2015). Process Analytical Technology (PAT) and Multivariate Methods for Downstream Processes. *Current Biochemical Engineering, 2*(1), 4-16.

Morrison, F. A. (2001). *Understanding Rheology.* New York: Oxford University Press.

Rasras, M., Elfadel, I. M., & Ngo, H. D. (2019). *MEMS Accelerometers.* Basel: MDPI.

Schwab, K. (2016, January 14). *The Fourth Industrial Revolution: what it means, how to respond.* Retrieved from https://www.weforum.org/agenda/2016/01/the-fourth-industrial-revolution-what-it-means-and-how-to-respond/

Tronci, S., Van Neer, P., Giling, E., Stelwagen, U., Piras, D., Mei, R., . . . Grosso, M. (2019). In-Line Monitoring and Control of Rheological Properties through Data-Driven Ultrasound Soft-Sensors. *Sensors, 19*(22).

Tzaneva, D., Djivoderova, M., Petkova, N., Denev, P., Hadzhikinov, D., & Stoyanova, A. (2017). Rheological Properties of the Cosmetic Gel Including Carboxymethyl Chitosan. *Journal of Pharmaceutical Sciences and Research*, *9*(8), 1383-1387.

Wang, Q. J., & Chung, Y. (2013). *Encyclopedia of Tribology.* New York: Springer Science.

Whitaker, M., Baker, G. R., Westrup, J., Goulding, P. A., Rudd, D. R., Belchamber, R. M., & Collins, M. P. (2000). Application of acoustic emission to the monitoring and end point determination of a high shear granulation process. *International Journal of Pharmaceutics*, *205*, 79-91.